Experimental investigation of methane hydrate formation in the presence of metallic packing

Experimental investigation of methane hydrate formation in the presence of metallic packing

Nithin B. Kummamuru[1], Sammy W. Verbruggen[1,4], Silvia Lenaerts[1,4], Patrice Perreault[2,3]*

[1]Sustainable Energy Air & Water Technology (DuEL), Department of Bioscience Engineering, University of Antwerp, Groenenborgerlaan 171, 2020 Antwerpen, Belgium.

[2]Faculty of Science, Instituut voor Milieu & Duurzame Ontwikkeling (IMDO), Campus Groenenborger – Building V.612, Groenenborgerlaan 171, 2020 Antwerpen, Belgium.

[3]University of Antwerp, BlueApp, Middelheimlaan 1, 2020 Antwerpen, Belgium

[4]NANOlab Center of Excellence, University of Antwerp, Groenenborgerlaan 171, 2020 Antwerpen, Belgium.

ABSTRACT

Clathrate hydrates gained significant attention as a viable option for large-scale storage of natural gas, primarily methane (CH_4). Unlike employing the nanoconfinement for enhancing the nucleation sites and hydrate growth as in the porous materials, whose synthesis is often associated with high costs and poor batch reproducibility, a new approach for promoting CH_4 hydrates using pure water (H_2O) in an unstirred reactor packed with stainless steel beads (SSB) was proposed in this fundamental work, where the interstitial space between the beads was exploited for enhanced hydrate growth. SSB of two diameters, 5 mm and 2 mm, were used as

20   a packed bed to investigate their effects on CH_4 hydrate formation at 273.65 K, 275.65 K, and

21   277.65 K with an initial pressure of 6 MPa. The thermal conductivity of SSB packing

22   potentially aided hydrate growth by expelling the hydration heat, while, the results also

23   revealed that driving force has a substantial impact on the rate of CH_4 hydrate formation and

24   gas uptake. The experiments conducted in both 5 mm and 2 mm SSB packed bed reactors

25   showed a maximum gas uptake of 0.147 mol CH_4/mol H_2O at 273.65 K with water to hydrate

26   conversion of 84.42% with no significant variation. The results established the promotion

27   effect on the kinetics of CH_4 hydrate formation in the unstirred reactor packed with 2 mm SSB

28   due to the availability of more interstitial space offering multiple nucleation sites for CH_4

29   hydrate by providing a larger specific surface area for H_2O-CH_4 reaction. Experiments with

30   varying H_2O content were also performed and the results showed that the water to hydrate

31   conversion and rate of hydrate formation could be enhanced at a lower H_2O content in a packed

32   bed reactor. This study demonstrates that the use of costly or intricate porous materials can be

33   made redundant, by exploiting the interstitial voids in packing of cheap and widely available

34   SSB as a promising alternative material for enhancing the kinetics of artificial CH_4 hydrate

35   synthesis.

36   KEYWORDS: methane hydrate, gas hydrates, hydrate formation, gas storage, fixed bed,

37   energy storage

38

39   1. Introduction

40   The demand for basic energy sources such as coal, oil, natural gas is increasing as a result of

41   rapid growth in population, industrial advancement, and transportation. The large depletion of

42   coal and oil reserves and carbon dioxide emissions associated with their use has shifted the

43   attention of governments and their energy policies towards utilizing natural gas and hydrogen

44   as an imperative condition for global environmental security[1-6]. Natural gas which is > 95

45   percent methane (CH_4), has been touted as an excellent alternative to coal and oil as a fuel for

46   power generations and transportation due to its low carbon emission characteristics such as

47   releasing considerably lesser degree of pollutants upon combustion per energy basis[7, 8].

48   Despite CH_4 being acknowledged as a potential energy source[9], the major challenge is in

49   its handling, and achieving high storage capacities both economically and safely. The

50   commercially available methods like liquified natural gas (LNG) and compressed natural gas

51   (CNG), which are capable of achieving predominant volumetric capacities ($\approx$ 600 v/v for LNG,

52    $\approx$ 240 v/v for CNG) and energy densities (22.2 MJ/l for LNG and 9 MJ/l for CNG[10]) greatly

53   suffer from their expensive cryogenic (113 K) and high-pressure (25 MPa) storage approaches

54   that prevent their widespread use[11-15]. In this light, another promising alternative technology

55   that gained significant attention for potential natural gas storage and transportation is the

56   formation of natural gas hydrates (NGHs)[16-19] and a comprehensive review of

57   advancements in gas hydrates research on challenges, limitations, and future perspective is

58   presented by Hassanpouryouzband et al.[20]. Gas hydrates or clathrate hydrates are

59   nonstoichiometric crystalline compounds that form at high pressures and low temperatures

60   when suitable sized gas molecules (CH_4 in this work; guest) are trapped in the cage structures

61   built by the hydrogen-bonded water (H_2O) molecules (host), where the trapped CH_4 molecules

62   stabilize the H_2O lattice via van der Waals forces[2, 21]. NGHs, primarily CH_4 hydrates can

63   deliver approximately 170 m^3 of CH_4 gas per unit volume at moderate storage conditions[2,

64   22, 23]. Alongside storage capacity, they are also considered safe because of their non-

65   explosive nature and cost-effectiveness compared to the commercial methods[24-27], but it is

66   also important to emphasize that gas leaks from clathrates can be unsafe in case of improper

67   storage and transport conditions. In addition to their natural gas storage application, hydrates

68   can be used for the capture of CO_2 from flue gases[28, 29], gas separation[30], refrigerants[31],

69   hydrogen storage[6], and water desalination[32]. However, the gas hydrate technology is not

70   yet industrially competitive with the existing storage and transport methods and is critically

71   challenged due to its low water-to-hydrate conversion, slow formation kinetics, and extremely

72   low temperatures to keep them stable at atmospheric pressure[33]. Most of these challenges

73   are caused by inadequate contact between gas/water (mass transfer) and the generation of large

74   hydrate heat which does not promote hydrate formation and growth[34]. Consequently,

75   enhancing the mass transfer and heat transfer by effective gas/water contact and removing the

76   hydration heat respectively are necessary for an efficient hydration process.

77   Tremendous research has been focused on overcoming the above-mentioned challenges by

78   employing mechanical methods such as stirring[35-44], gas bubbling[45-47], and spraying[48-

79   51], however, some drawbacks associated with these approaches hinder them for practical

80   applications. Mechanical agitation in a stirred tank reactor is a matured and conventional

81   technique. Despite advantages such as shorter induction times and faster hydrate formation

82   rates at early stages[52], stirred tank reactors have a disadvantage of limited conversion of

83   water and gas to hydrates due to agglomeration of hydrate crystals; acting as a barrier that

84   prevents efficient contact between gas and liquid[53, 54]. Other disadvantages are the

85   decomposition of hydrates over long-term stirring[42], the high energy cost for stirring upon

86   thickening of hydrate slurry[35, 45], and inconvenience in separating the produced hydrates on

87   a continuous production scale[55]. Besides mechanical stirring, the major underlying problem

88   in spray reactors is the ineffective cooling upon hydrate formation[56]. Another alternative

89   approach is the use of bubble tower reactors that have the advantage of better contact between

90   gas and liquid, at the same time suffer from disadvantages like separation of formed hydrate at

91   the gas/liquid interface and limited heat transfer rates during hydrate formation[45]. Though

92   the rate of hydrate formation is high on a fresh bubble, the hydrate shells at a later stage were

93   found to agglomerate rather than merging into bigger bubbles and hindering further hydrate

94 formation. A comprehensive review on reactor design and their associated challenges upon

95 scaling up is presented by A. Gupta et al.[6] and Y. H. Mori[57].

96 Aside from new reactor designs, continuous research efforts have been communicated[9, 58-

97 75] in enhancing the kinetics of CH_4 hydrate formation by the use of thermodynamic promoters

98 or kinetic promoters (predominantly surfactants), where these surfactants reduce the interfacial

99 tension between (guest) gas-liquid (host) interface and enhance the hydrate growth (mass

100 transfer of gas and liquid phase) without affecting the thermodynamics[67, 68]. Nevertheless,

101 fast hydrate formation is always associated with high hydration heat which ultimately weakens

102 the acceleration effect of surfactants on hydrate formation[77, 78]. On the other hand, the

103 thermodynamic promoters which can alter the hydrate forming conditions, predominantly

104 occupy the larger cages of the hydrate and eventually lower the CH_4 storage capacity compared

105 to pure CH_4 hydrates, consequently a penalty on storage capacity is ineludible[71]. A

106 comprehensive list of both kinetic and thermodynamic promoters for CH_4 hydrates is presented

107 in our earlier publication[9].

108 Another alternative approach to enhance the kinetics of CH_4 hydrate formation rate is by

109 employing a fixed bed porous column without stirring and some of the existing research has

110 already shed light on suitable fixed bed packings to enhance water-to-hydrate conversion and

111 to boost the hydrate growth[25, 44, 76, 78-141]. Developing a synthetic porous material with

112 high storage capacity, high chemical, mechanical and thermal stability is assumed to be vital

113 for a successful and efficient storage process. Research is currently advancing in determining

114 such potential porous materials and some of them (including but not limited to) that are actively

115 pursued are carbon-based porous materials[25, 91, 142-144], silica-based materials[88, 94,

116 107, 141, 145-149], zeolites[122, 150-153], metal-organic frameworks[100, 120, 143, 154-

117 156]. Aside from the development of new synthetic methods, it is also important to mention

118 that mass production of these materials for large-scale applications is often associated with

119 high costs and poor reproducibility between batches[15, 157, 158]. Although a significant

120 amount of research has shown interest in the hydrate mass transfer rate, the constraints of heat

121 transfer have largely been overlooked although it plays a crucial role in potential scale-up. In

122 view of the latter, relatively limited studies[77, 159-174] have been conducted to enhance the

123 thermal conductivity of hydrate systems utilizing novel materials together with kinetic

124 promoters. More recently, open-cell aluminum metal, SiC foam with good thermal

125 conductivity was used to enhance the removal rate of hydration heat through the cell walls and

126 increase the CH_4 hydrate formation rate[76, 98, 175]. Similarly, stainless steel structured

127 packing in presence of a kinetic promoter was also used as a fixed-bed medium to enhance the

128 thermal conductivity of the bed for CO_2 hydrates[176].

129 Inspired by this, we used stainless steel beads (SSB) as a fixed-bed porous column for CH_4

130 enclathration in this study. Up till now, to our knowledge, there is no report in the literature

131 concerning how SSB packing affects the CH_4 hydrate formation and with this in mind, we

132 evaluate the effect of CH_4 hydrate formation kinetics in pure water at different temperatures

133 and constant pressure in presence of an SSB packed bed. Furthermore, the SSB packing can

134 enhance the thermal conductivity of the bed, concurrently, the thermal conductivity of stainless

135 steel beads (~14.6 W m^{-1} K^{-1})[177] being approximately 24 to 25 times higher than that of CH_4

136 hydrate (~0.60 W m^{-1} K^{-1})[178-180] can potentially accelerate hydrate growth by rapidly

137 removing the hydrate heat from the reaction. Accordingly, the kinetics of CH_4 hydrate

138 formation in presence of SSB packing, the effects of water content on gas uptake, and water to

139 hydrate conversions are also evaluated.

140
141 2. Experimental section

142 2.1 Experimental apparatus

143 As shown in Figure 1, the CH_4 hydrate formation experiments were carried out in cylindrical

144 stainless steel (SS) reactor (diameter: 48.3 mm, height: 20.3 mm, effective volume: 150 cm^3)

145   purchased from Swagelok (316L-50DF4-150) with a pressure rating of 34.4 MPa. To obtain a

146   stable temperature and to control the temperature precisely, the SS reactor was immersed in a

147   high-precision circulating bath (CORIO CP-1000F, JULABO GmbH) filled with a water-

148   ethylene glycol mixture. The temperature stability of the bath was ± 0.03 K. The pressure

149   within the reactor was monitored by connecting a pressure transmitter (PAA3X-300bar;

150   KELLER AG; a range of 0-300 bar absolute) having an accuracy of ± 0.01% FS. A data

151   acquisition system connected with a computer was used to record the temperature and pressure

152   every 1 second. Stainless steel beads of diameters 5 mm and 2 mm, purchased from IKA^{TM}

153   (Fisher Scientific platform) were used as the fixed-bed porous medium. Methane gas (99.99%

154   purity) used in this study was supplied by Air Liquide Benelux Industries and deionized water

155   with a resistivity of 18 mΩ.cm^{-1} was made in the laboratory.

156   2.2 Experimental procedure

157   A standard approach was used to measure the formation of CH_4 hydrates at constant volume

158   and the experimental procedure may be described as follows. Prior to the experiments, the SS

159   316L reactor was cleaned with deionized water and dried with compressed air, followed by

160   packing the reactor with cleaned (with H_2O) and dried stainless-steel beads along with the

161   required volume of deionized water. Subsequently, the reactor was purged with CH_4 gas (0.2

162   MPa) 10 times to remove any residual air in the system. The reactor was then immersed in the

163   water-ethylene glycol bath (temperature: ~303 K) and CH_4 gas is injected slowly into the

164   reactor to a pressure of 6 MPa. Concurrently, the data acquisition started to record the bath

165   temperature and pressure inside the reactor at a 1 Hz frequency. The reactor was kept at this

166   steady ambient temperature to prevent any hydrate formation. After the temperature and

167   pressure being stabilized, the reactor was then cooled down to the experimental temperature,

168   and the time when these thermodynamic conditions, the temperature, and pressure of the

169   reactor reached the experimental conditions was considered as time zero. The hydrate

170 formation was considered to be complete when a pressure drop of less than 0.02 MPa in 30

171 min was observed. It is also important to mention that the measurements were performed with

172 an identical reference vessel (with SSB, but in absence of water) having the same configuration

173 as the actual hydrate formation reactor (sample reactor). Each experiment was repeated two

174 times. In this work, the amount of CH_4 gas consumed was used to determine the extent of CH_4

175 hydrate formed. The dissolution of CH_4 gas was not considered in the current study due to its

176 low solubility[141, 181] in water at these temperatures, and also the solubility of CH_4 being

177 very small it can be neglected when compared to the amount of CH_4 consumed for hydrate

178 formation. The gas consumption was calculated using the compressibility factor equation of

179 state. The moles of CH_4 gas consumed during hydrate formation were calculated using (Eq. 1),

$$\Delta n_{hyd} = V_r \left(\frac{P_i}{Z_i RT} - \frac{P_t}{Z_t RT} \right) \qquad \text{(Eq. 1)}$$

180 where, Δn_{hyd} is the moles of CH_4 gas consumed at time t, V_r is the volume of gas-phase

181 inside the reactor measured using helium expansion method[182, 183], P_i is the initial pressure

182 of hydrate formation stage, P_t is the pressure of hydrate formation stage at time t in the reactor,

183 R is the ideal gas constant, T is the temperature of the reactor, Z_i is the compressibility of gas

184 at the start of hydrate formation and Z_t is compressibility factor of gas in the reactor at time t.

185 The compressibility factors Z_i and Z_t are calculated using the Pitzer correlation[184]. The

186 percentage of water to hydrate conversion ($C_{WH}(mol \%)$) is determined using (Eq. 2), and the

187 normalized gas (NG_t) uptake at any given time t is calculated using (Eq. 3),

$$C_{WH}(mol \%) = \frac{\Delta n_{hyd} \times hydration\ number}{n_{H2O}} \times 100 \qquad \text{(Eq. 2)}$$

188

$$NG_t = \frac{\Delta n_{hyd}}{n_{H2O}} \ (mol\ of\ gas\ /\ mol\ of\ water) \qquad \text{(Eq. 3)}$$

189

190 where, n_{H2O} are the total number of moles of H_2O in the system and hydration number is

191 defined as the number of H_2O molecules required to encapsulate one guest (CH_4) molecule,

192 and the water-to-hydrate conversion in this work was calculated assuming the hydration

193 number as 5.75[99, 133, 185]. A discrete first-order forward difference method was used to

194 calculate the rate of CH_4 hydrate formation as shown in (Eq. 4), where Δt is the time difference

195 between two observations.

$$\frac{dN_t}{dt} = \left(\frac{d\Delta n_{hyd}}{dt} \right) \approx \frac{\Delta n_{hyd,t+\Delta t} - \Delta n_{hyd,t}}{\Delta t}, \Delta t = 2\ mins \qquad \text{(Eq. 4)}$$

196

197 Stainless steel beads (SSB) of diameters 5 mm and 2 mm were used as packing medium in

198 the reactor to study the characteristics of the hydrate formation process. All the experiments

199 were conducted by filling the reactor with 2.05 g H_2O and the experiments were carried out at

200 an initial pressure of 6 MPa, and temperatures 273.65 K, 275.65 K, 277.65 K. As it is known

201 that a larger driving force can favor (shorten) the hydrate formation induction time[36, 186] at

202 a given temperature or pressure, this work sets the experimental pressure (P_{exp}) at 6 MPa. The

203 CH_4 hydrate formation phase equilibrium curve from CSMHYD[187] and Kummamuru et

204 al.[9] reports hydrate equilibrium pressure (P_{eq}) approximately at 2.7 MPa, 3.3 MPa, 4 MPa at

205 273.65 K, 275.65 K, and 277.65 K respectively. Therefore, the driving force ($\Delta P = P_{exp} - P_{eq}$;

206 at a given temperature) for hydrate formation in this work was calculated to be 3.3 MPa, 2.7

207 MPa, and 2 MPa for the three selected temperatures, respectively.

208

209 3. Results and discussion

210 Table 1. summarizes the CH_4 hydrate experimental results from this work including

211 maximum growth rate, water-to-hydrate conversion percentage at 273.65 K, 275.65 K, 277.65

212 K in 5 mm and 2 mm SSB packed bed systems. Figure 2. shows the CH_4 uptake profile during

213 hydrate formation in SSB (5 mm) packing at 273.65 K. An average gas uptake plot from three

214 experiments is shown along with the standard deviation and time zero corresponding to the

215 nucleation point for the experiment. As seen in the figure, a maximum uptake of 0.147 mol

216 CH_4/mol H_2O was achieved in 140 min, and as a comparison at these thermodynamic

217 conditions (273.65 K and 6 MPa), CH_4 gas solubility in H_2O is approximately 0.002 mol

218 CH_4/mol H_2O according to NIST database[188], indicating that it is fair to assume the gas

219 uptake is almost exclusively due to CH_4 enclathration in H_2O cages during hydrate formation.

220 SSB being non-porous, the possible explanation for CH_4 hydrate formation is the presence of

221 a higher driving force coupled with nucleation sites provided by the interstitial space between

222 SSB, which eventually promoted hydrate nucleation and aided further growth. Reports by Jin

223 et al.[189], Linga et al.[88] also support the current findings, where CH_4 hydrate has been

224 reported to form in the interstitial area between sand particles. Aside from providing nucleation

225 sites via interstitial space, the SSB packing may have also offered the service of rapid hydrate

226 heat transfer, which accelerated hydrate formation. Maximum water-to-hydrate conversion in

227 SSB (5 mm) packing and at these thermodynamic conditions was found to be approximately

228 84.4% in 140 min of hydrate growth. The inset in Figure 2. presents the gas uptake

229 measurements for the experiments conducted at 275.65 K and 277.65 K in a 5 mm SSB packed

230 bed filled with 2.05g H_2O. As can be seen, with an increase in temperature, the normalized gas

231 uptake decreased, where a maximum uptake of 0.137 mol CH_4/mol H_2O was achieved at

232 275.65 K in 525 min whereas it took approximately 3 times longer to reach a maximum gas

233 uptake of 0.094 CH_4/mol H_2O at 277.65 K compared to 275.65 K.

234 Figure 3. compares CH_4 hydrate growth rate in the 5 mm SSB packed bed at all the three

235 temperatures studied in this work for the first 140 min. An average gas uptake from three

236 experiments is shown along with the standard deviation and time zero corresponds to the

237 nucleation point for all of the experiments conducted. It can be seen that the rate of hydrate

238 formation increases as the temperature decreases, which clearly indicates the direct influence

239   of increased driving force. A maximum gas uptake of 0.069 mol CH_4/mol H_2O was achieved

240   at 275.65 K and 0.049 mol CH_4/mol H_2O at 277.65 K in 140 min, which is only 46.9% and

241   33% of the measured gas uptake at 273.65 K, respectively.

242   The effect of particle size on CH_4 hydrate formation was also investigated at the lowest

243   temperature of 273.65 K and 6 MPa by packing the reactor with 2 mm SSB. Figure 4. compares

244   the hydrate formation behavior in 5 mm and 2 mm SSB packing reactor filled with 2.05 g H_2O.

245   It can be observed that the experiments conducted with small SSB and large SSB, provide

246   almost identical maximal gas uptake values with no significant variation. However, it can be

247   deduced that the 2 mm SSB packing medium enhanced the rate of methane hydrate formation

248   due to the availability of more interstitial space (as a result of decreased beads size) which offer

249   multiple nucleation sites for CH_4 gas hydrate by providing a larger specific surface area relative

250   to 5 mm SSB packing which also improved the contact between gas-liquid-solid to be a priority

251   site for hydrate nucleation[125, 141, 190, 191]. Rapid hydrate growth is always associated with

252   the swift release of hydration heat. Aside from providing hydrate nucleation sites, the thermal

253   conductivity of 2 mm SSB packing may have enhanced hydrate formation by rapidly expelling

254   the hydration heat. A closer examination at the normalized gas uptake at the 10th min already

255   shows 0.119 mol CH_4/mol H_2O for 2 mm SSB packing, while 5 mm SSB packing at the same

256   time shows 70.58% lower uptake, reading 0.035 mol CH_4/mol H_2O.

257   Attempting to compare the performance of SSB packing with other reported packed bed

258   materials for promoting CH_4 hydrate formation could be of potential interest. However, merely

259   comparing the absolute values of hydrate growth rate, maximum stored capacity, water to

260   hydrate conversion drawn from various laboratories, methods and reactors may not be a reliable

261   way to determine which one leapfrogged the other. Such for instance, P. Hu et al.[115] and M.

262   Zi et al.[192] reported that any change in the microstructure of high-pressure metal made

263   reactor surfaces (roughness) would tremendously affect the hydrate growth rate which

264 subsequently affects water to hydrate conversion as well as induction time. In this regard, it is

265 also important to mention that most of the high-pressure reactors reported in the literature were

266 made of metal material. Furthermore, different experimental procedures can also have

267 significant effects on hydrate growth rate or induction time, for instance, in some of the

268 studies[115, 193] as well as in the present study, the hydrate forming gas (e.g. CH_4) was

269 introduced into the reactor before reaching the experimental temperature, contrarily, in other

270 studies[175, 194, 195], the hydrate forming gas is introduced into the reactor upon reacting the

271 experimental temperature. Compared with former conditions, both the hydrate gas dissolution

272 and nucleation may occur concurrently in latter conditions, which substantially narrows the

273 induction time. However, it is exemplary to make a comparison between the works using fixed

274 packing as the case in this study that has larger particle diameters providing nucleation sites

275 for hydrate formation. As shown in Figure 5, only the works[107, 141, 196-199] using fixed

276 packing materials having particle diameters greater than 1 mm were selected for comparison.

277 The results demonstrated that the water to hydrate conversion reported in previous studies

278 ranged from 16.8% to 84.43%, while the maximum water to hydrate conversion was upto

279 84.42% with 5 mm or 2 mm SSB packing employed in the present study. In comparison, the

280 water to hydrate conversion (84.43%) reported by Filarsky et al.[107] is relatively similar to

281 the conversion (84.2%) presented in this study, however, it is worth mentioning that the

282 experimental pressure employed in their study is two times higher than the pressure used in the

283 present work. In contrast to this work, it should also be emphasized that many of the studies

284 presented in Figure 5. used kinetic promoters to enhance the hydrate formation rate.

285 The rate of CH_4 hydrate formation in 5 mm SSB packing with the driving force of 3.3 MPa,

286 2.7 MPa, 2 MPa is presented in Figure 6. As can be seen, the rate of hydrate growth is higher

287 for the system with a larger driving force, followed by the other two driving forces in

288 decreasing order. For instance, at 2 min of hydrate growth, the rate is 3.28 times and 8.61 times

289 higher in the larger driving force (3.3 MPa) than in other driving force conditions 2.3 MPa and

290 2 MPa respectively. For the system with the larger driving force, the rate slows down and

291 reaches nearly zero in 140 min. Similarly, the rate of CH_4 hydrate formation in 2 mm SSB

292 packing and 5 mm SSB packing studies conducted at a driving force of 3.3 MPa are compared

293 in Figure 7. For smaller SSB packing, the rate of hydrate formation is relatively higher than the

294 larger SSB packing. In the first 10 min, a rapid hydrate rate can be observed in smaller SSB

295 packing followed by a gradual decrease and reaching zero in about 40 min indicating the

296 completion of hydrate formation, while the rate continues in larger SSB packing up till 140

297 min.

298 Additionally, the mass of H_2O in the reactor was varied and investigated to evaluate the

299 influence of H_2O content on hydrate formation. Figure 8. shows the gas uptake measurements

300 for the experiments conducted at 273.65 K and 275.65 K in a 5 mm SSB packed bed filled with

301 10.25 g H_2O and with an initial pressure of 6 MPa. As can be seen, the maximum gas uptake

302 achieved after 1794 min is 0.054 mol CH_4/mol H_2O at 273.65 K and 0.035 mol CH_4/mol H_2O

303 at 275.65 K. These results clearly show a decrease in gas uptake with an increase in H_2O

304 content from 2.05 g to 10.25 g. For instance, the gas uptake value for 10.25 g H_2O at the lowest

305 operating temperature in 5 mm SSB packing is 81.16% lower compared to that achieved with

306 2.05 g H_2O within the first 140 min. This infers that the rate of hydrate formation, water-to-

307 hydrate conversion could be accelerated when the water content is lower in a packed bed and

308 this is always relative to the amount of H_2O used[89, 132, 200]. Figure 9. compares the

309 normalized gas uptake measurements for the experiments conducted at 273.65 K and 275.65

310 K in a 5 mm SSB packed bed filled with 2.05 g and 10.25 g H_2O. It can be seen that experiments

311 performed with larger H_2O content were able to achieve approximately 30% of gas uptake at

312 similar thermodynamic conditions for lower H_2O content and the corresponding low rate of

313 hydrate formation can be seen in Figure S1. Comprehensively, this study highlights that SSB

314   packing can foster CH_4 hydrate formation at the thermodynamic pressures of 6 MPa and

315   temperatures over 273.15 K, as well as enhance hydrate growth at lower H_2O saturations by

316   altering the packing size.

317

318   4. Conclusion

319   The formation behavior of CH_4 hydrate in an unstirred reactor packed with different sizes of

320   stainless steel beads (SSB) was investigated in this study at three different temperatures of

321   273.65 K, 275.65 K, 277.65 K with a starting experimental pressure of 6 MPa. The results

322   demonstrated that both types of SSB employed in this study as the packing medium effectively

323   promoted hydrate formation and, in addition to offering nucleation sites, the thermal

324   conductivity of SSB conceivably favored by expelling the hydration heat. A maximum gas

325   uptake of 0.147 mol CH_4/mol H_2O was achieved at 273.65 K in 140 min in a 5 mm SSB packed

326   bed filled with 2.05 g H_2O. The experiments conducted at 273.65 K and 2.05 g H_2O in an

327   unstirred reactor packed with 2 mm SSB showed a higher rate compared to the reactor packed

328   with 5 mm SSB. However, the maximum water-to-hydrate conversion achieved in both

329   systems is similar, and approximately 84.42%. The smaller size SSB packing medium

330   effectively accelerated the CH_4 hydrate growth rate at an early stage due to the availability of

331   more interstitial space offering multiple nucleation sites for gas hydrate by providing a larger

332   specific surface area for water-gas reaction. A maximum gas uptake of 0.147 mol CH_4/mol

333   H_2O was achieved in 95 min which was approximately 45 min faster than for reaching a similar

334   gas uptake value in a 5 mm SSB packed bed reactor. This highlights the requirement for

335   optimizing the structure of the packed bed reactor to improve the contact between gas-liquid-

336   solid to be a priority site for hydrate nucleation. In addition, the influence of H_2O content on

337   hydrate formation was also evaluated in the 5 mm SSB packed bed reactor at 273.65 K and

338   275.65 K. The maximum water-to-hydrate conversion of 30.87% was achieved only after 1794

339 min of hydrate formation for 10.25 g of H_2O saturation at 273.65 K. In this vein, at a lower

340 H_2O saturation, it can be speculated that the surface contact area between the two phases (gas-

341 liquid) increased, resulting in rapid hydrate formation and gas consumption. Furthermore, it

342 can be deduced that tuning the H_2O saturation in a packed bed can maximize the rate of hydrate

343 formation and gas uptake. Conclusively, the results from this work could potentially eliminate

344 the porous material synthesis cost and the need for stirring, both of which are economically

345 beneficial, while also being a promising alternative material for enhancing CH_4 hydrate

346 synthesis in comparison to the extensive research on porous materials reported in the literature.

347 The findings from this work are also expected to be beneficial for large-scale natural gas

348 storage in the form of hydrates within a packed metal bed.

349

350 **Corresponding author***

351 Patrice.Perreault@uantwerpen.be Tel: +32 456 16 27 33

352

353 **ORCID**

354 Nithin B. Kummamuru: 0000-0003-2989-3079

355 Patrice Perreault: 0000-0002-9392-2113

356 Sammy W. Verbruggern: 0000-0003-2372-9630

357 Silvia Lenaerts: 0000-0003-4314-9676

358

359 **Notes**

360 The authors declare no competing financial interest.

361 **Supporting Information**

362 **The supporting information is available free of charge on the ACS Publications website**
363 **at DOI:**

364 Rate of CH_4 hydrate formation conducted at 273.65 K and 275.65 K in a 5 mm SSB packed

365 bed filled with 10.25 g H_2O

366   References

367   [1]   Sloan ED, Fundamental principles and applications of natural gas hydrates, Nature 426
368   (2003) 353-359.
369   [2]   Sloan ED, Koh CA, Clathrate hydrates of natural gases, CRC Press, 2007.
370   [3]   Khan MI, Policy options for the sustainable development of natural gas as a
371   transportation fuel, Energy Policy 110 (2017) 126-136.
372   [4]   Pratson LF, Haerer D, Patino-Echeverri D, Fuel prices, emission standards, and
373   genaration costs for coal vs natural gas power plants, Environ. Sci. Technol. 47 (2013)
374   4926-4933.
375   [5]   Arutyunov VS, Lisichkin GV, Energy resources of the 21st century: problems and
376   forecasts. can renewable energy sources replace fossil fuels?, Russ. Chem. Rev. 86
377   (2017) 777-804.
378   [6]   Gupta A, Baron GV, Perreault P, Lenaerts S, Ciocarlan RG, Cool P, et al., Hydrogen
379   clathrates: Next generation hydrogen storage materials, Energy Storage Mater. 41
380   (2021) 69-107.
381   [7]   Celzard A, Fierro V, Preparing a suitable material designed for methane storage: a
382   comprehensive report, Energy Fuels 19 (2005) 573-583.
383   [8]   Balasubramanian V, Energy sources: Fundamentals of chemical processes and
384   applications, Elsevier B.V., 2017, pp. 59-79.
385   [9]   Kummamuru NB, Perreault P, Lenaerts S, A new generalized empirical correlation for
386   predicting methane hydrate equilibrium conditions in pure water, Ind. Eng. Chem. Res.
387   60 (2021) 3474-3483.
388   [10]   Mazloomi K, Gomes C, Hydrogen as an energy carrier: prospects and challenges,
389   Renew. Sust. Energ. Rev. 16 (2012) 3024-3033.
390   [11]   Mahboub MJD, Ahmadpour A, Rashidi H, Improving methane storage on wet activated
391   carbons at various amounts of water, J. Fuel Chem. Technol. 40 (2012) 385-389.
392   [12]   Alhasan S, Carriveau R, Ting DSK, A review of adsorbed natural gas storage
393   technologies, Int. J. Environ. Stud. 73 (2016) 343-356.
394   [13]   Quinn DF, MacDonald JA, Natural gas storage, Carbon 30 (1992) 1097-1103.
395   [14]   McTaggart-Cowan GP, Reynolds CCO, Bushe WK, Natural gas fuelling for heavy-
396   duty on-road use: current trends and future direction, Int. J. Environ. Stud. 63 (2006)
397   421-440.
398   [15]   Makal TA, Li J, Lu W, Zhou HC, Methane storage in advanced porous materials, Chem.
399   Soc. Rev. 41 (2012) 7761-7779.
400   [16]   Johnson AH, The development path for hydrate natural gas, Proceedings of the 6th
401   international conference on gas hydrates (ICGH 2008), Vancouver, 2008.
402   [17]   Nogami T, Oya N, Development of natural gas ocean transportation chain by means of
403   natural gas hydrate (NGH), Proceedings of the 6th international conference on gas
404   hydrates (ICGH 2008), Vancouver, 2008.
405   [18]   Lee SY, Holder GD, Methane hydrates potential as a future energy source, Fuel
406   Process. Technol. 71 (2001) 181-186.
407   [19]   Makogon YF, Holditch SA, Makogon TY, Natural gas-hydrates — a potential energy
408   source for the 21st century, J. Pet. Sci. Eng. 56 (2007) 14-31.
409   [20]   Hassanpouryouzband A, Joonaki E, Farahni MV, Takeya S, Ruppel C, Yang J, et al.,
410   Gas hydrates in sustainable chemistry, Chem. Soc. Rev. 49 (2020) 5525-5309.
411   [21]   Koh CA, Towards a fundamental understanding of natural gas hydrates, Chem. Soc.
412   Rev. 31 (2002) 157-167.

413 [22] Song YC, Yang L, Zhao JF, Liu WG, Yang MJ, Li YH, et al., The status of natural gas
414   hydrate research in China: A review, Renewable Sustainable Energy Rev. 31 (2014)
415   778-791.
416 [23] Englezos P, Lee JD, Gas hydrates: A cleaner source of energy and opportunity for
417   innovative technologies, KoreanJ. Chem. Eng. 22 (2005) 671-681.
418 [24] Stern LA, Circone S, Kirby SH, Durham WB, Anomalous preservation of pure methane
419   hydrate, J. Phys. Chem. B 105 (2001) 1756-1762.
420 [25] Casco ME, Zhang E, Grätz S, Krause S, Bon V, Wallacher D, et al., Experimental
421   evidence of confined methane hydrate in hydrophilic and hydrophobic model carbons,
422   J. Phys. Chem. C 123 (2019) 24071-24079.
423 [26] Zhang G SM, Liu B, Wang F, Adsorption-induced two-way nanoconvection enhances
424   nucleation and growth kinetics of methane hydrates in confined porespace, Chem. Eng.
425   J. 396 (2020) 125256.
426 [27] Zhang G, Shi X, Zhang R, Chao K, Wang F, Promotion of activated carbon on the
427   nucleation and growth kinetics of methane hydrates, Front. Chem. 8 (2020) 934.
428 [28] Hassanpouryouzband A, Yang J, Tohidi B, Chuvilin E, Istomin V, Bukhanov B, et al.,
429   Insights into CO_2 capture by flue gas hydrate formation: Gas composition evolution in
430   systems containing gas hydrates and gas mixtures at stable pressures, ACS Sustainable
431   Chem. Eng. 6 (2018) 5732-5736.
432 [29] Hassanpouryouzband A, Yang J, Tohidi B, Chuvilin E, Istomin V, Bukhanov B,
433   Geological CO_2 capture and storage with flue gas hydrate formation in frozen and
434   unfrozen sediments: Method development, real time-scale kinetic characteristics,
435   efficiency, and clathrate structural transition, ACS Sustainable Chem. Eng. 7 (2019)
436   5338-5345.
437 [30] Babu P, Linga P, Kumar R, Englezos, P, A review of the hydrate based gas separation
438   (HBGS) process for carbon dioxide pre-combustion capture, Energy 85 (2015) 261-
439   279.
440 [31] Hashemi H, Babaee S, Mohammadi AH, Naidoo P, Ramjugernath D, State of the art
441   and kinetics of refrigerant hydrate formation, Int. J. Refrig. 98 (2019) 410-427.
442 [32] Kang KC, Linga P, Park K, Choi S, Lee JD, Seawater desalination by gas hydrate
443   process anr removal characteristics of dissolved ions (Na^+, K^+, Mg^{2+}, Ca^{2+}, B^{3+}, Cl^-,
444   SO_4^{2-}), Desalination. 353 (2014) 84-90.
445 [33] Lang X, Fan S, Wang Y, Intensification of methane and hydrogen storage in clathrate
446   hydrate and future prospect, J. Nat. Gas Chem. 19 (2010) 203-209.
447 [34] Aman ZM, Koh CA, Interfacial phenomena in gas hydrate systems, Chem. Soc. Rev.
448   45 (2016) 1678-1690.
449 [35] Vysniauskas A, Bishnoi PR, A kinetic study of methane hydrate formation, Chem. Eng.
450   Sci. 38 (1983) 1061-1072.
451 [36] Skovborg P, Ng HJ, Rasmussen P, Mohn U, Measurement of induction times for the
452   formation of methane and ethane gas hydrates, Chem. Eng. Sci. 48 (1993) 445-453.
453 [37] Kim NJ, Lee JH, Cho YS, Chun W, Formation enhancement of methane hydrate for
454   natural gas transport and storage, Energy 35 (2010) 2717-2722.
455 [38] Linga P, Kumar R, Lee JD, Ripmeester J, Englezos P, A new apparatus to enhance the
456   rate of gas hydrate formation: application to capture of carbon dioxide, Int. J. Greenh.
457   Gas Control. 4 (2010) 630-637.
458 [39] Dufour T, Hoang HM, Oignet J, Osswald V, Clain P, Fournaison L, et al., Impact of
459   pressure on the dynamic behavior of CO_2 hydrate slurry in a stirred tank reactor applied
460   to cold thermal energy storage, Appl. Energy 204 (2017) 641-652.
461 [40] Du JW, Li HJ, Wang LG, Cooperative effect of surfactant addition and gas-inducing
462   agitation on methane hydrate formation rate, Fuel 230 (2018) 134-137.

[41] Azam MZ, Xin F, Song Y, Qaraah FAA, Abbas SZ, Rate enhancement of methane hydration in slurry of ice by phase change of water-in-oil emulsions, Fuel 244 (2019) 296-303.

[42] Hao WF, Wang JQ, Fan SS, Hao WB, Study on methane hydration process in a semi-continuous stirred tank reactor, Energy Convers. Manage. 48 (2007) 954-960.

[43] Veluswamy HP, Kumar A, Kumar R, Linga P, An innovative approach to enhance methane hydrate formation kinetics with leucine for energy storage application, Appl. Energy 188 (2017) 190-199.

[44] Linga P, Daraboina N, Ripmeester JA, Englezos P, Enhanced rate of gas hydrate formation in a fixed bed column filled with sand compared to a stirred vessel, Chem. Eng. Sci. 68 (2012) 617-623.

[45] Luo YT, Zhu JH, Fan SS, Chen GJ, Study on the kinetics of hydrate formation in a bubble column, Chem. Eng. Sci. 62 (2007) 1000-1009.

[46] Fu WQ, Wang ZY, Sun BJ, Chen LT, A mass transfer model for hydrate formation in bubbly flow considering bubble-bubble interactions and bubble-hydrate particle interactions, Int. J. Heat Mass Transf. 127 (2018) 611-621.

[47] Lv QN, Li XS, Xu CG, Chen ZY, Experimental investigation of the formation of cyclopentane-methane hydrate in a novel and large-size bubble column reactor, Ind. Eng. Chem. Res. 51 (2012) 5967-5975.

[48] Fukumoto K, Tobe J, Ohmura R, Mori YH, Hydrate formation using water spraying in a hydrophobic gas: a preliminary study, AlChE J. 47 (2001) 1899-1904.

[49] Fujita S, Watanabe K, Mori YH, Clathrate-hydrate formation by water spraying onto a porous metal plate exuding a hydrophobic liquid coolant, AlChE J. 55 (2009) 1056-1064.

[50] Partoon B, Sabil KM, Lau KK, Lal B, Nasrifar K, Production of gas hydrate in a semi-batch spray reactor process as a means for separation of carbon dioxide from methane, Chem. Eng. Res. Des. 138 (2018) 168-175.

[51] Tsuji H, Ohmura R, Mori YH, Forming structure-H hydrates using water spraying in methane gas: effects of chemical species of large-molecule guest substances, Energy Fuels 18 (2004) 418-424.

[52] He Y, Rudolph ESJ, Zitha PLJ, Golombok M, Kinetics of CO_2 and methane hydrate formation: An experimental analysis in the bulk phase, Fuel 90 (2011) 272-279.

[53] Englezos P, Nucleation and growth of gas hydrate crystals in relation to kinetic inhibition, Rev. IFP 51 (1996) 789.

[54] Lee JD, Susilo R, Englezos P, Kinetics of structure H gas hydrate, Energy Fuels 19 (2005) 1008-1015.

[55] Rossi F, Filipponi M, Castellani B, Investigation on a novel reactor for gas hydrate production, Appl. Energy 99 (2012) 167-172.

[56] Tsuda SMH, Mori YH, Hydrate formation using water spraying onto a cooled solid surface in a guest gas, AlChE J. 52 (2006) 2978-2987.

[57] Mori YH, On the scale-up of gas-hydrate-forming reactors: The case of gas-dispersion-type reactors, Energies 8 (2015) 1317-1335.

[58] Zhong Y, Rogers RE, Surfactant effects on gas hydrate formation, Chem. Eng. Sci. 55 (2000) 4175-4187.

[59] Kumar A, Bhattacharjee G, Kulkarni BD, Kumar R, Role of surfactants in promoting gas hydrate formation, Ind. Eng. Chem. Res. 54 (2015) 12217-12232.

[60] He Y, Sun MT, Chen C, Zhang GD, Chao K, Lina Y, et al., Surfactant-based promotion to gas hydrate formation for energy storage, J. Mater. Chem. A 7 (2019) 21634-21661.

511	[61]	Lin W, Chen GJ, Sun CY, Guo XQ, Wu ZK, Liang MY, et al., Effect of surfactant on
512		the formation and dissociation kinetic behavior of methane hydrate, Chem. Eng. Sci.
513		59 (2004) 4449-4455.
514	[62]	Wang F, Jia ZZ, Luo SJ, Fu SF, Wang L, Shi XS, et al., Effects of different anionic
515		surfactants on methane hydrate formation, Chem. Eng. Sci. 137 (2015) 896-903.
516	[63]	Kim S, Baek IH, You JK, Seo Y, Guest gas enclathration in tetran-butyl ammonium
517		chloride (TBAC) semiclathrates: potential application to natural gas storage and CO_2
518		capture, Appl. Energy 140 (2015) 107-112.
519	[64]	Liao ZX, Guo XQ, Li Q, Sun Q, Li J, Yang LY, et al., Experimental and modeling
520		study on the phase equilibria for hydrates of gas mixtures in TBAB solution, Chem.
521		Eng. Sci. 137 (2015) 656-664.
522	[65]	Nasir Q, Suleman H, Elsheikh YA, A review on the role and impact of various additives
523		as promoters/ inhibitors for gas hydrate formation, Int. J. Greenh. Gas Control. 76
524		(2020) 103211.
525	[66]	Kumar A, Veluswamy HP, Kumar R, Linga P, Kinetic promotion of mixed methane-
526		THF hydrate by additives: Opportune to energy storage, Energy procedia 158 (2019)
527		5287-5292.
528	[67]	Kalogerakis N, Jamaluddin AKM, Dholabhai PD, Bishnoi PR, Effect of surfactants on
529		hydrate formation kinetics, SPE International Symposium on Oilfield Chemistry, New
530		Orleans, Louisiana, 1993.
531	[68]	Karaaslan U, Parlaktuna M, Surfactants as hydrate promoter?, Energy Fuels 14 (2000)
532		1103-1107.
533	[69]	Shi LL, Ding JX, Liang DQ, Enhanced CH_4 storage in hydrates with the presence of
534		sucrose stearate, Energy 180 (2019) 978-988.
535	[70]	Yoslim J, Linga P, Englezos P, Enhanced growth of methane–propane clathrate hydrate
536		crystals with sodium dodecyl sulfate, sodium tetradecyl sulfate, and sodium hexadecyl
537		sulfate surfactants, J. Cryst. Growth 313 (2010) 68-80.
538	[71]	Veluswamy HP, Kumar S, Kumar R, Rangsunvigit P, Linga P, Enhanced clathrate
539		hydrate formation kinetics at near ambient temperatures and moderate pressures:
540		Application to natural gas storage, Fuel 182 (2016) 907-919.
541	[72]	Brinchi L, Castellani B, Rossi F, Cotana F, Morini E, Nicolini A, et al., Experimental
542		investigations on scaled-up methane hydrate production with surfactant promotion:
543		energy considerations, J. Pet. Sci. Eng. 120 (2014) 187-193.
544	[73]	Sun ZG, Wang R, Ma R, Guo K, Fan S, Natural gas storage in hydrates with the
545		presence of promoters, Energy Convers Manage 44 (2003) 2733-2742.
546	[74]	Ganji H, Manteghian M, Sadaghiani KZ, Omidkhah MR, Rahimi HM, Effect of
547		different surfactants on methane hydrate formation rate, stability and storage capacity,
548		Fuel 86 (2007) 434-441.
549	[75]	Ando N, Kuwabara Y, Mori YH, Surfactant effects on hydrate formation in an unstirred
550		gas/liquid system: an experimental study using methane and micelle-forming
551		surfactants, Chem. Eng. Sci. 73 (2012) 79-85.
552	[76]	Fan S, Yang L, Lang X, Wang Y, Xie D, Kinetics and thermal analysis of methane
553		hydrate formation in aluminum foam, Chem. Eng. Sci. 82 (2012) 185-193.
554	[77]	Yang L, Wang X, Liu D, Cui G, Dou B, Wang J, et al., Accelerated methane storage in
555		clathrate hydrates using surfactantstabilized suspension with graphite nanoparticles,
556		Chin. J. Chem. Eng. 28 (2020) 1112-1119.
557	[78]	Kumar A, Sakpal T, Linga P, Kumar R, Influence of contact medium and surfactants
558		on carbon dioxide clathrate hydrate kinetics, Fuel 105 (2013) 664-671.

559   [79]   Kumar A, Sakpal T, Linga P, Kumar R, Enhanced carbon dioxide hydrate formation
560   kinetics in a fixed bed reactor filled with metallic packing, Chem. Eng. Sci. 122 (2015)
561   78-85.

562   [80]   Seo YT, Moudrakovski IL, Ripmeester JA, Lee JW, Lee H, Efficient recovery of CO_2
563   from flue gas by clathrate hydrate formation in porous silica gels, Environ. Sci.
564   Technol. 39 (2005) 2315-2319.

565   [81]   Ho LC, Babu P, Kumar R, Linga P, HBGS (hydrate based gas separation) process for
566   carbon dioxide capture employing an unstirred reactor with cyclopentane, Energy 63
567   (2013) 252-259.

568   [82]   Kang SP, Lee J, Seo Y, Pre-combustion capture of CO_2 by gas hydrate formation in
569   silica gel pore structure, Chem. Eng. J. 218 (2013) 126-132.

570   [83]   Babu P, Kumar R, Linga P, A new porous material to enhance the kinetics of clathrate
571   process: Application to precombustion carbon dioxide capture, Environ. Sci. Technol.
572   47 (2013) 13191-13198.

573   [84]   Babu P, Kumar R, Linga P, Pre-combustion capture of carbon dioxide in a fixed bed
574   reactor using the clathrate hydrate process, Energy 50 (2013) 364-373.

575   [85]   Liu J, Ding JX, Liang DQ, Experimental study on hydrate-based gas separation of
576   mixed CH_4/CO_2 using unstable ice in a silica gel bed, Energy 157 (2018) 54-64.

577   [86]   Kang SP, Seo Y, Jang W, Kinetics of methane and carbon dioxide hydrate formation in
578   silica gel pores, Energy Fuels 23 (2009) 3711-3715.

579   [87]   Kang SP, Lee WJ, Formation characteristics of synthesized natural gas hydrates in
580   meso and macroporous silica gels, J. Phys. Chem. B 114 (2010) 6973-3978.

581   [88]   Linga P, Haligva C, Nam SC, Ripmeester JA, Englezos P, Gas hydrate formation in a
582   variable volume bed of silica sand particles, Energy Fuels 23 (2009) 5496-5507.

583   [89]   Bagherzadeh SA, Moudrakovski IL, Ripmeester JA, Englezos P, Magnetic resonance
584   imaging of gas hydrate formation in a bed of silica sand particles, Energy Fuels 25
585   (2011) 3083-3092.

586   [90]   Linga P, Haligva C, Nam SC, Ripmeester JA, Englezos P, Recovery of methane from
587   hydrate formed in a variable volume bed of silica sand particles, Energy Fuels 23 (2009)
588   5508-5516.

589   [91]   Casco ME, Albero JS, Ramírez-Cuesta AJ, Rey F, Jordá JL, Bansode A, et al., Methane
590   hydrate formation in confined nanospace can surpass nature, Nat. Commun. 6 (2015)
591   6432.

592   [92]   Park SS, Lee SB, Kim NJ, Effect of multi-walled carbon nanotubes on methane hydrate
593   formation, J. Ind. Eng. Chem. 16 (2010) 551-555.

594   [93]   Celzard A, Marêché JF, Optimal wetting of active carbons for methane hydrate
595   formation, Fuel 85 (2006) 957-966.

596   [94]   Uchida T, Ebinuma T, Ishizaki T, Dissociation condition measurements of methane
597   hydrate in confined small pores of porous glass, J. Phys. Chem. B 103 (1999) 3659-
598   3662.

599   [95]   Zhang Y, Zhao Y, Lei X, Yang M, Zhang Y, Song Y, Quantitatively study on methane
600   hydrate formation/decomposition, Fuel 262 (2020) 116555.

601   [96]   Fitzgerald GC, Castaldi M, Schicks JM, Methane hydrate formation and thermal based
602   dissociation behavior in silica glass bead porous media, Ind. Eng. Chem. Res. 53 (2014)
603   6840-6854.

604   [97]   Ge BB, Zhong DL, Lu YY, Influence of water saturation and particle size on methane
605   hydrate formation and dissociation in a fixed bed of silica sand, Energy procedia 157
606   (2019) 5402-5407.

607   [98]   Liu X, Tian L, Chen D, Wu G, Accelerated formation of methane hydrates in the porous
608   SiC foam ceramic packed reactor, Fuel 257 (2019) 115858.

609 [99]   Prasad PSR, Sowjanya Y, Chari VD, Enhancement in methane storage capacity in gas
610   hydrates formed in hollow silica, J. Phys. Chem. C 118 (2014) 7759-7764.
611 [100] Casco ME, Rey F, Jordá JL, Rudić S, Fauth F, Escandell MM, et al., Paving the way
612   for methane hydrate formation on metal−organic frameworks (MOFs), Chem. Sci. 7
613   (2016) 3658-3666.
614 [101] Wang WX, Bray CL, Adams DJ, Cooper AI, Methane storage in dry water gas hydrates,
615   J. Am. Chem. Soc. 130 (2008) 11608-11609.
616 [102] Carter BO, Wang WX, Adams DJ, Cooper AI, Gas storage in ″dry water″ and ″dry gel″
617   clathrates, Langmuir 26 (2010) 3186-3193.
618 [103] Wang JL, Wang RJ, Yoon RH, Seol Y, Use of hydrophobic particles as kinetic
619   promoters for gas hydrate formation, J. Chem. Eng. Data 60 (2015) 383-388.
620 [104] Li HJ, Wang LG, Hydrophobized particles can accelerate nucleation of clathrate
621   hydrates, Fuel 140 (2015) 440-445.
622 [105] Guo Y, Xiao W, Pu W, Hu J, Zhao J, Zhang L, CH_4 nanobubbles on the hydrophobic
623   solid−water interface serving as the nucleation sites of methane hydrate, Langmuir 34
624   (2018) 10181-10186.
625 [106] Wang R, Liu T, Ning F, Ou W, Zhang L, Wang Z, et al., Effect of hydrophilic silica
626   nanoparticles on hydrate formation: Insight from the experimental study, J. Energy
627   Chem. 30 (2019) 90-100.
628 [107] Filarsky F, Schmuck C, Schultz HJ, Impact of modified silica beads on methane hydrate
629   formation in a fixed-bed reactor, Ind. Eng. Chem. Res. 58 (2019) 16687-16695.
630 [108] Yangsheng Z, Jianzhong Z, Dinxian S, Zengchao F, Weiguo L, Dong Y, Micro-CT
631   analysis of structural characteristics of natural gas hydrate in porous media during
632   decomposition, J. Nat. Gas Sci. Eng. 31 (2016) 139-148.
633 [109] Zhou Y, Wang Y, Chen H, Zhou L, Methane storage in wet activated carbon: studies
634   on the charging/discharging process, Carbon 43 (2005) 2007-2012.
635 [110] Liu J, Zhou Y, Sun Y, Su W, Zhou L, Methane storage in wet carbon of tailored pore
636   sizes, Carbon 49 (2011) 3731-3736.
637 [111] Zhou L, Liu J, Su W, Sun Y, Zhou Y, Progress in studies of natural gas storage with
638   wet adsorbents, Energy Fuels 24 (2010) 3789-3795.
639 [112] Veluswamy HP, Prasad PSR, Linga P, Mechanism of methane hydrate formation in the
640   presence of hollow silica, KoreanJ. Chem. Eng. 33 (2016) 2050-2062.
641 [113] Zhao J, Zhao Y, Liang W, Song S, Gao Q, Semi-clathrate hydrate process of methane
642   in porous media-mesoporous materials of SBA-15, Fuel 220 (2018) 446-452.
643 [114] Chen LT, Li N, Sun CY, Chen GJ, Koh CA, Sun BJ, Hydrate formation in sediments
644   from free gas using a one-dimensional visual simulator, Fuel 197 (2017) 298-309.
645 [115] Hu P, Chen D, Zi M, Wu G, Effects of carbon steel corrosion on the methane hydrate
646   formation and dissociation, Fuel 230 (2018) 126-133.
647 [116] Shi BH, Yang L, Fan SS, Lou X, An investigation on repeated methane hydrates
648   formation in porous hydrogel particles, Fuel 194 (2017) 395-405.
649 [117] Wang W, Jiang K, Li Y, Shi Z, Song G, Duan R, Kinetics of methane gas hydrate
650   formation with microscale sand in an autoclave with windows, Fuel 209 (2017) 85-95.
651 [118] Saw VK, Udayabhanu G, Mandal A, Laik S, Methane hydrate formation and
652   dissociation in the presence of silica sand and bentonite clay, Oil & Gas Science and
653   Technology – Rev. IFP Energies nouvelles 70 (2014) 1087-1099.
654 [119] Perrin A, Celzard A MJ, Furdin G, Improved methane storage capacities by sorption on
655   wet active carbons, Carbon 42 (2004) 1249-1256.
656 [120] Mu L, Liu B, Liu H, Yang Y, Sun C, Chen G, A novel method to improve the gas
657   storage capacity of ZIF-8, J. Mater. Chem. 22 (2012) 12246-12252.

658 [121] Zhou L, Sun Y, Zhou YP, Enhancement of the methane storage on activated carbon by
659   pre-adsorbed water, AlChE J. 48 (2002) 2412-2416.
660 [122] Andres-Garcia E, Dikhtiarenko A, Fauth F, Silvestre-Albero J, Ramos-Fernández EV,
661   Gascon J, et al., Methane hydrates: nucleation in microporous materials, Chem. Eng. J.
662   360 (2019) 569-576.
663 [123] Wang PF, Yang MJ, Chen BB, Zhao YC, Zhao JF, Song YC, Methane hydrate
664   reformation in porous media with methane migration, Chem. Eng. Sci. 168 (2017) 344-
665   351.
666 [124] Uchida T, Ebinuma T, Takeya S, Nagao J, Narita H, Effects of pore sizes on
667   dissociation temperatures and pressures of methane, carbon dioxide, and propane
668   hydrates in porous media, J. Phys. Chem. B 106 (2002) 820-826.
669 [125] Siangsai A, Rangsunvigit P, Kitiyanan B, Kulprathipanja S, Linga P, Investigation on
670   the roles of activated carbon particle sizes on methane hydrate formation and
671   dissociation, Chem. Eng. Sci. 126 (2015) 383-389.
672 [126] Babu P, Yee D, Linga P, Palmer A, Khoo BC, Tan TS, et al., Morphology of methane
673   hydrate formation in porous media, Energy Fuels 27 (2013) 3364-3372.
674 [127] Kneafsey TJ, Tomutsa L, Moridis GJ, Seol Y, Freifeld BM, Taylor CE, et al., Methane
675   hydrate formation and dissociation in a partially saturated core-scale sand sample, J.
676   Pet. Sci. Eng. 56 (2007) 108-126.
677 [128] Choi J-H, Dai S, Cha J-H, Seol Y, Laboratory formation of noncementing hydrates in
678   sandy sediments, Geochem. Geophys. Geosystems 15 (2014) 1648-1656.
679 [129] Mekala P, Babu P, Sangwai JS, Linga P, Formation and dissociation kinetics of
680   methane hydrates in seawater and silica sand, Energy Fuels 28 (2014) 2708-2716.
681 [130] Li FG, Sun CY, Zhang Q, Liu XX, Guo XQ, Chen GJ, Laboratory measurements of the
682   effects of methane/tetrahydrofuran concentration and grain size on the p-wave velocity
683   of hydrate-bearing sand., Energy Fuels 25 (2011) 2076-2082.
684 [131] Sun SC, Liu CL, Ye YG, Liu YF, Phase behavior of methane hydrate in silica sand, J.
685   Chem. Thermodyn. 69 (2014) 118-124.
686 [132] Kumar A, Sakpal T, Roy S, Kumar R, Methane hydrate formation in a test sediment of
687   sand and clay at various levels of water saturation, Can. J. Chem. 93 (2015) 874-881.
688 [133] Chari VD, Sharma DVSGK, Prasad PSR, Murthy SR, Methane hydrates formation and
689   dissociation in nano silica suspension, J. Nat. Gas Sci. Eng. 11 (2013) 7-11.
690 [134] Ding A, Yang L, Fan S, Lou X, Reversible methane storage in porous hydrogel
691   supported clathrates, Chem. Eng. Sci. 96 (2013) 124-130.
692 [135] Veluswamy HP, Kumar A, Seo Y, Lee JD, Linga P, A review of solidified natural gas
693   (SNG) technology for gas storage via clathrate hydrates, Appl. Energy 216 (2018) 262-
694   285.
695 [136] Palodkar AV, Jana AK, Clathrate hydrate dynamics with synthetic and bio-surfactant
696   in porous media: model formulation and validation, Chem. Eng. Sci. 213 (2020)
697   115386.
698 [137] Zhang B, Zheng J, Yin Z, Liu C, Wu Q, Wu Q, et al., Methane hydrate formation in
699   mixed-size porous media with gas circulation: Effects of sediment properties on gas
700   consumption, hydrate saturation and rate constant, Fuel 233 (2018) 94-102.
701 [138] Liu J, Liang D, Investigation on methane hydrate formation in silica gel particles below
702   the freezing point, RSC Adv. 9 (2019) 15022.
703 [139] Collados CC, Pérez JF, Escandell MM, Missyul A, Albero JS, Effect of additives in the
704   nucleation and growth of methane hydrates confined in a high-surface area activated
705   carbon material, Chem. Eng. J. 388 (2020) 124224.

706 [140] Liu H, Zhan S, Guo P, Fan S, Zhang S, Understanding the characteristic of methane
707   hydrate equilibrium in materials and its potential application, Chem. Eng. J. 349 (2018)
708   775-781.
709 [141] Chong ZR, Yang M, Khoo BC, Linga P, Size effect of porous media on methane
710   hydrate formation and dissociation in an excess gas environment, Ind. Eng. Chem. Res.
711   55 (2016) 7981-7991.
712 [142] Cuadrado-Collados C, Fauth F, Such-Basanez I, Martinez-Escandell M, Silvestre-
713   Albero J, Methane hydrate formation in the confined nanospace of activated carbons in
714   seawater environment, Micropor. Mesopor. Mat. 255 (2018) 220-225.
715 [143] Borchardt L, Casco ME, Silvestre-Albero J, Methane hydrate in confined spaces: An
716   alternative storage system, ChemPhysChem 19 (2018) 1298-1314.
717 [144] Liu J, Wei Y, Meng W, Li PZ, Zhao Y, Zou R, Understanding the pathway of gas
718   hydrate formation with porous materials for enhanced gas separation, Research 2019
719   (2019) 3206024.
720 [145] Nair VC, Ramesh S, Ramadass GA, Sangwai JS, Influence of thermal stimulation on
721   the methane hydrate dissociation in porous media under confined reservoir, J. Pet. Sci.
722   Eng. 147 (2016) 547-559.
723 [146] Handa YP, Stupin DY, Thermodynamic properties and dissociation characteristics of
724   methane and propane hydrates in 70-.ANG.-radius silica gel pores, J. Phys. Chem. 96
725   (1992) 8599-8603.
726 [147] Seo Y, Lee H, Uchida T, Methane and carbon dioxide hydrate phase behavior in small
727   porous silica gels: three-phase equilibrium determination and thermodynamic
728   modeling, Langmuir 18 (2002) 9164-9170.
729 [148] Inkong K, Veluswamy HP, Rangsunvigit P, Kulprathipanja S, Linga P, Innovative
730   approach to enhance the methane hydrate formation at near-ambient temperature and
731   moderate pressure for gas storage applications, Ind. Eng. Chem. Res. 58 (2019) 22178-
732   22192.
733 [149] Smith DH, Wilder JW, Seshadri K, Methane hydrate equilibria in silica gels with broad
734   pore-size distributions, AIChE J. 48 (2004) 393-400.
735 [150] Kim NJ, Park SS, Shin SW, Hyun JH, Chun W, Phase equilibria of CO_2 and CH_4
736   hydrates in intergranular meso/macro pores of MIL-53 metal organic framework, Int.
737   J. Energy Res. 39 (2014) 26-32.
738 [151] Zang X, Du J, Liang D, Fan S, Tang C, Influence of A-type zeolite on methane hydrate
739   formation, Chin. J. Chem. Eng. 17 (2009) 854-859.
740 [152] Zhong DL, Li Z, Lu YY, Wang JL, Yan J, Qing SL, Investigation of CO_2 capture from
741   a CO_2 + CH_4 gas mixture by gas hydrate formation in the fixed bed of a molecular
742   sieve, Ind. Eng. Chem. Res. 55 (2016) 7973-7980.
743 [153] Zhao Y, Zhao J, Liang W, Gao Q, Yang D, Semi-clathrate hydrate process of methane
744   in porous media-microporous materials of 5A-type zeolites, Fuel 220 (2018) 185-191.
745 [154] Denning S, Majid AA, Lucero JM, Crawford JM, Carreon MA, Koh CA, Metal–
746   Organic Framework HKUST-1 promotes methane hydrate formation for improved gas
747   storage capacity, ACS Appl. Mater. Interfaces 12 (2020) 53510-53518.
748 [155] Cuadrado-Collados C, Mouchaham G, Daemen L, Cheng Y, Ramirez-Cuesta A,
749   Aggarwal H, et al., Quest for an optimal methane hydrate formation in the pores of
750   hydrolytically stable metal–organic frameworks, J. Am. Chem. Soc. 142 (2020) 13391-
751   13397.
752 [156] Kim D, Ahn YH, Lee H, Phase equilibria of CO_2 and CH_4 hydrates in intergranular
753   meso/macro pores of MIL-53 metal organic framework, J. Chem. Eng. Data 60 (2015)
754   2178-2185.

755 [157] Rubio-Martinez M, Avci-Camur C, Thornton AW, Imaz I, Maspoch D, Hill MR, New
756 synthetic routes towards MOF production at scale, Chem. Soc. Rev. 46 (2017) 3453-
757 3480.
758 [158] DeSantis D, Mason JA, James BD, Houchins C, Long JR, Veenstra M, Techno-
759 economic analysis of metal-organic frameworks for hydrogen and natural gas storage,
760 Energy Fuels 31 (2017) 2024-2032.
761 [159] Zhang G, Zhang R, Wang F, Fast formation kinetics of methane hydrates loaded by
762 silver nanoparticle coated activated carbon (Ag-NP@AC), Chem. Eng. J. 417 (2021)
763 129206.
764 [160] Yang L, Liu Z, Liu D, Cui G, Dou B, Wang J, et al., Enhanced natural gas hydrates
765 formation in the suspension with metal particles and fibers, J. Mol. Liq. 301 (2020)
766 112410.
767 [161] Song YM, Wang F, Guo G, Luo SJ, Guo RB, Energy-efficient storage of methane in
768 the formed hydrates with metal nanoparticles-grafted carbon nanotubes as promoter,
769 Appl. Energy 224 (2018) 175-183.
770 [162] Nashed O, Partoon B, Lal B, Sabil KM, Shariff AM, Review the impact of nanoparticles
771 on the thermodynamics and kinetics of gas hydrate formation, J. Nat. Gas Sci. Eng. 55
772 (2018) 452-465.
773 [163] Abkenar MR, Manteghian M, Pahlavanzadeh H, Experimental and theoretical
774 investigation of methane hydrate induction time in the presence of triangular silver
775 nanoparticles, Chem. Eng. Res. Des. 120 (2017) 325-332.
776 [164] Liu GQ, Wang F, Luo SJ, Xu DY, Guo RB, Enhanced methane hydrate formation with
777 SDS-coated Fe_3O_4 nanoparticles as promoters, J. Mol. Liq. 230 (2017) 315-321.
778 [165] Li DL, Peng H, Liang DQ, Thermal conductivity enhancement of clathrate hydrate with
779 nanoparticles, Int. J. Heat Mass Tran. 104 (2017) 566-573.
780 [166] Said S, Govindaraj V, Herri JM, Ouabbas Y, Khodja M, Belloum M, et al., Study on
781 the influence of nanofluid on gas hydrate formation kinetics and their potential:
782 application to the CO_2 capture process, J. Nat. Gas Sci. Eng. 32 (2016) 95-108.
783 [167] Mohammadi M, Haghtalab A, Fahkroueian Z, Experiential study and thermodynamic
784 modeling of CO_2 gas hydrate formation in presence of zinc oxide nanoparticles, J.
785 Chem. Thermodyn. 96 (2016) 24-33.
786 [168] Najibi H, Shayegan MM, Heidary H, Experimental investigation of methane hydrate
787 formation in the presence of copper oxide nanoparticles and SDS, J. Nat. Gas Sci. Eng.
788 23 (2015) 315-323.
789 [169] Arjang S, Manteghian M, Mohammadi A, Effect of synthesized silver nanoparticles in
790 promoting methane hydrate formation at 4.7 MPa and 5.7 MPa, Chem. Eng. Res. Des.
791 91 (2013) 1050-1054.
792 [170] Mohammadi A, Manteghian M, Mohammadi AH, Jahangiri A, Induction time, storage
793 capacity, and rate of methane hydrate formation in the presence of SDS and silver
794 nanoparticles, Chem. Eng. Commun. 204 (2017) 1420-1427.
795 [171] Mohammadi A, Effect of SDS, silver nanoparticles, and SDS + silver nanoparticles on
796 methane hydrate semicompletion time, Pet. Sci. Technol. 35 (2017) 1542-1548.
797 [172] Wang F, Sum AK, Liu B, Recent advances in promoters for gas hydrate formation
798 Front. Chem. 9 (2021) 708269.
799 [173] Pahlavanzadeh H, Rezaei S, Khanlarkhani M, Manteghian M, Mohammadi AH,
800 Kinetic study of methane hydrate formation in the presence of coppernanoparticles and
801 CTAB, J. Nat. Gas Sci. Eng. 34 (2016) 803-810.
802 [174] Wu Y, Tang T, Shi L, He Y, Rapid hydrate-based methane storage promoted by bilayer
803 surfactant-coated Fe_3O_4 nanoparticles under a magnetic field, Fuel 303 (2021) 121248.

[175] Yang L, Fan SS, Wang YH, Lang XM, Xie DL, Accelerated formation of methane hydrate in aluminum foam, Ind. Eng. Chem. Res. 50 (2011) 11563-11569.

[176] Kumar A, Kumar R, Role of metallic packing and kinetic promoter in designing a hydrate-based gas separation process, Energy Fuels 29 (2015) 4463-4471.

[177] Franssen JM, Real PV, Fire design of steel structures, ECCS - European Convention for Constructional Steelwork, 2013.

[178] Huang DZ, Fan SS, Liang DQ, Feng ZP, Gas hydrate formation and its thermal conductivity measurement, Chin. J. Geophys. 48 (2005) 1201-1207.

[179] Waite WF, Stern LA, Kirby SH, Winters WJ, Mason DH, Simultaneous determination of thermal conductivity, thermal diffusivity and specific heat in sI methane hydrate, Geophys. J. Int. 169 (2007) 767-774.

[180] English NJ, Tse JS, Perspectives on hydrate thermal conductivity, Energies 3 (2010) 1934-1942.

[181] Koh CA, Sum A, Sloan ED, Natural gas hydrates in flow assurance, Gulf Professional Publishing, 2010.

[182] Zou J, Rezaee R, Effect of particle size on high-pressure methane adsorption of coal, Pet. Res. 1 (2016) 53-58.

[183] Carrillo-Bucio JL, Tena-Garcia JR, Armenta-Garcia EP, Hernandez-Silva O, Cabañas-Moreno JG, Suárez-Alcántara K, Low-cost sieverts-type apparatus for the study of hydriding/dehydriding reactions, HardwareX 4 (2018).

[184] Smith JM, Ness HV, Abbott M, Swihart M, Introduction to chemical engineering thermodynamics, 8 ed., McGraw-Hill Education, 2015.

[185] Prasad PSR, Kiran BS, Sowjanya K, Enhanced methane gas storage in the form of hydrates: role of the confined water molecules in silica powders, RSC Adv. 10 (2020) 17795-17804.

[186] Natarajan V, Bishnoi PR, Kalogerakis N, Induction phenomena in gas hydrate nucleation, Chem. Eng. Sci. 49 (1994) 2075-2087.

[187] Sloan ED, CSMHYD, 1998.

[188] Linstrom PJ, Mallard WG, NIST Chemistry WebBook, NIST Standard Reference Database Number 69, National Institute of Standards and Technology, Gaithersburg MD, 20899.

[189] Jin Y, Konno Y, Nagao J, Growth of methane clathrate hydrates in porous media, Energy Fuels 26 (2012) 2242-2247.

[190] Liu Z, Pan Z, Zhang Z, Liu P, Shang L, Li B, Effect of porous media and sodium dodecyl sulphate complex system on methane hydrate formation, Energy Fuels 32 (2018) 5736-5749.

[191] Phirani J, Pitchumani R, Mohanty KK, History matching of hydrate formation and dissociation experiments in porous media, SPE Reservoir Simulation Symposium, Texas, 2009.

[192] Zi M, Chen D, Wu G, Molecular dynamics simulation of methane hydrate formation on metal surface with oil, Chem. Eng. Sci. 191 (2018) 253-261.

[193] Park T, Lee JY, Kwon TH, Effect of pore size distribution on dissociation temperature depression and phase boundary shift of gas hydrate in various fine-grained sediments, Energy Fuels 32 (2018) 5321-5330.

[194] Fan S, Yang L, Wang Y, Lang X, Wen Y, Lou X, Rapid and high capacity methane storage in clathrate hydrates using surfactant dry solution, Chem. Eng. Sci. 106 (2014) 53-59.

[195] Wang F, Guo G, Liu GQ, Luo SJ, Guo RB, Effects of surfactant micelles and surfactant-coated nanospheres on methane hydrate growth pattern, Chem. Eng. Sci. 144 (2016) 108-115.

854 [196] Qin Y, Bao R, Shang L, Zhou L, Meng L, Zang C, et al., Effects of particle size and
855   types of porous media on the formation and occurrence of methane hydrate in complex
856   systems, Energy Fuels 36 (2022) 655-668.
857 [197] Heydari A, Peyvandi K, Role of metallic porous media and surfactant on kinetics of
858   methane hydrate formation and capacity of gas storage, J. Pet. Sci. Eng. 181 (2019)
859   106235.
860 [198] Zhao J, Yang L, Liu Y, Song Y, Microstructural characteristics of natural gas hydrates
861   hosted in various sand sediments, Phys. Chem. Chem. Phys. 17 (2015) 22632.
862 [199] Zhao J, Lv Q, Li Y, Yang M, Liu W, Yao L, et al., In-situ visual observation for the
863   formation and dissociation of methane hydrates in porous media by magnetic resonance
864   imaging, Magn. Reson. Imaging 33 (2015) 485-490.
865 [200] Babu P, Kumar R, Linga P, Medium pressure hydrate based gas separation (HBGS)
866   process for pre-combustion capture of carbon dioxide employing a novel fixed bed
867   reactor, Int. J. Greenh. Gas Control. 17 (2013) 206-214.

868

Table 1. Summary of CH$_4$ hydrate formation at different experimental conditions in this study with P_{exp} of 6 MPa

System	T_{exp} (K)	Driving force (MPa)	end of experiment		NG_{t90} (mol CH$_4$/mol H$_2$O)	end of experiment	[a]V_H (cm^3)
			Time (min)	NG_t (mol CH$_4$/mol H$_2$O)		C_{WH} (mol%)	
5 mm SSB	273.65	3.3	140	0.147	0.117	84.42	1.92
packed bed +	275.65	2.7	525	0.137	0.057	79.00	1.79
2.05g H$_2$O	277.65	2	1545	0.094	0.042	53.84	1.22
5 mm SSB	273.65	2.7	1794	0.054	0.024	30.87	3.51
packed bed +	275.65	2	1794	0.035	0.014	20.13	2.30
10.25g H$_2$O							
2 mm SSB							
packed bed +	273.65	3.3	95	0.147	0.146	84.42	1.92
2.05g H$_2$O							

[a]volume of hydrate at the end of the experiment.
The density of CH$_4$ hydrate is assumed as 0.9 g.cm^{-3}.
$VH = \frac{m_{wc}}{0.9}$; $m_{wc} = \Delta n_{hyd} \times M_w \times hydration\ number$.
m_{wc} = mass of water consumed and M_w = molar mass of water
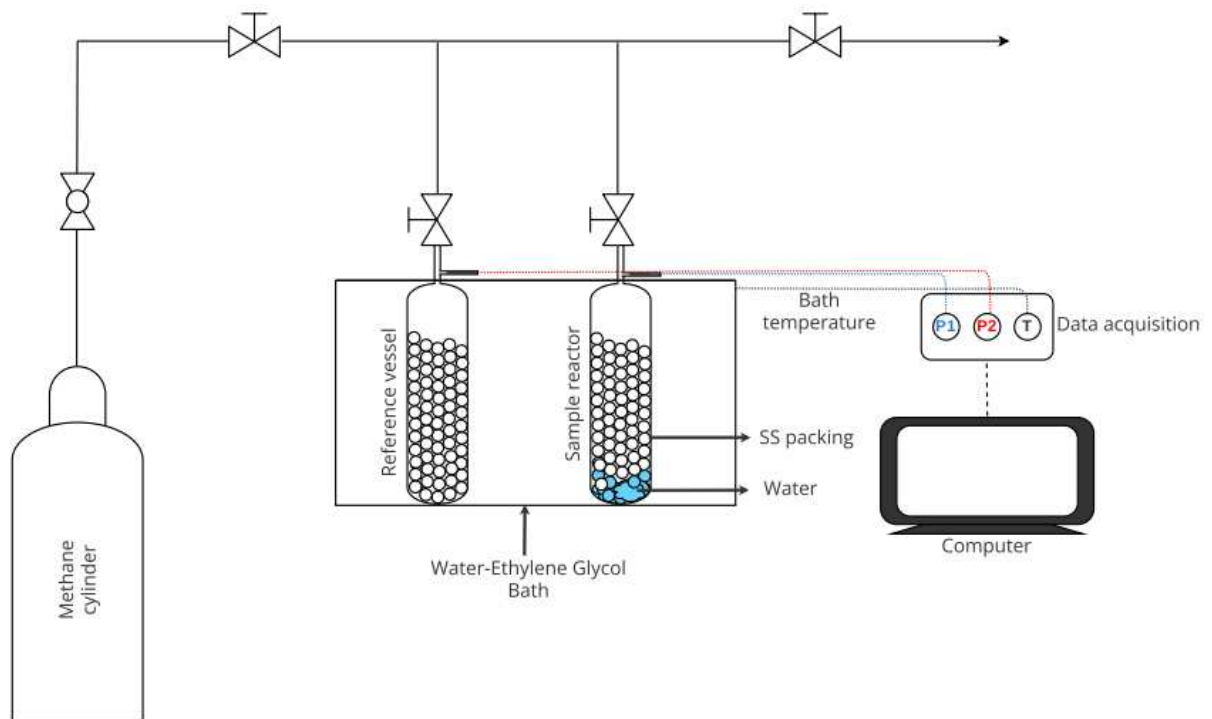
Figure 1. The schematic of the experimental setup for the study of CH$_4$ hydrate formation in SSB packing media
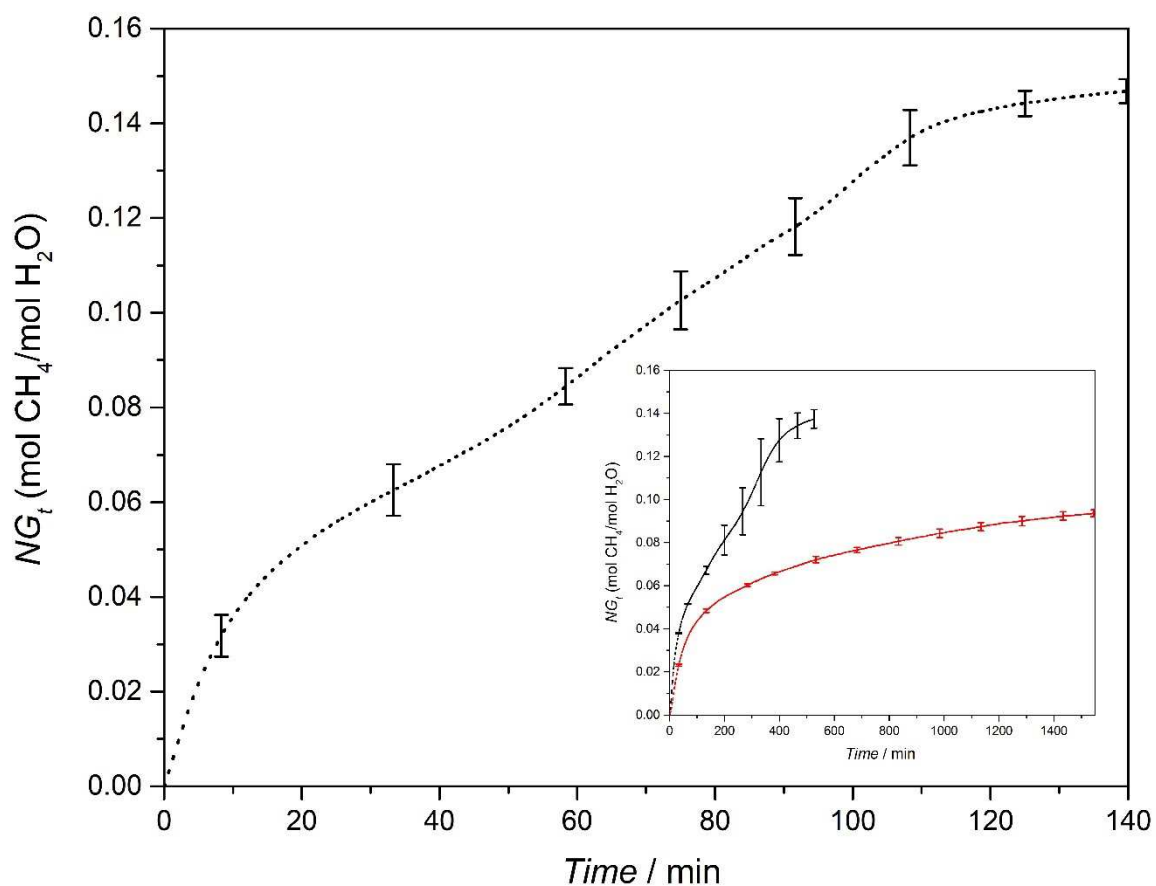
Figure 2. Average CH₄ uptake profile during hydrate formation experiments conducted at 273.65 K in a 5 mm SSB packed bed filled with 2.05g H$_2$O. Time zero corresponds to nucleation point. Inset: Average CH₄ uptake profile during hydrate formation experiments conducted at 275.65 K (black) and 277.65 K (red)
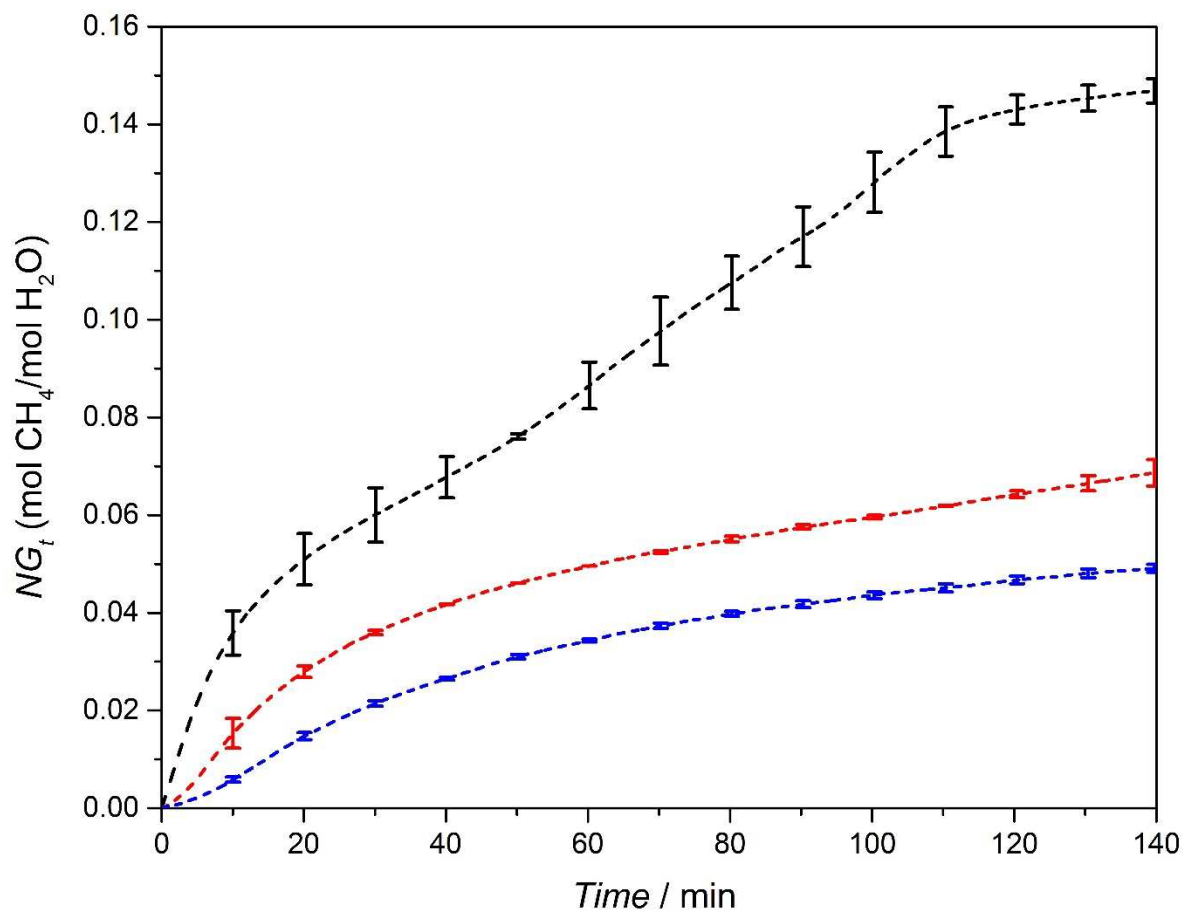
Figure 3. Comparison of average CH_4 uptake profile during hydrate formation experiments conducted at 273.65 K (black) and 275.65 K (red) 277.65 K (blue) in a 5 mm SSB packed bed filled with 2.05g H_2O. Time zero corresponds to nucleation point
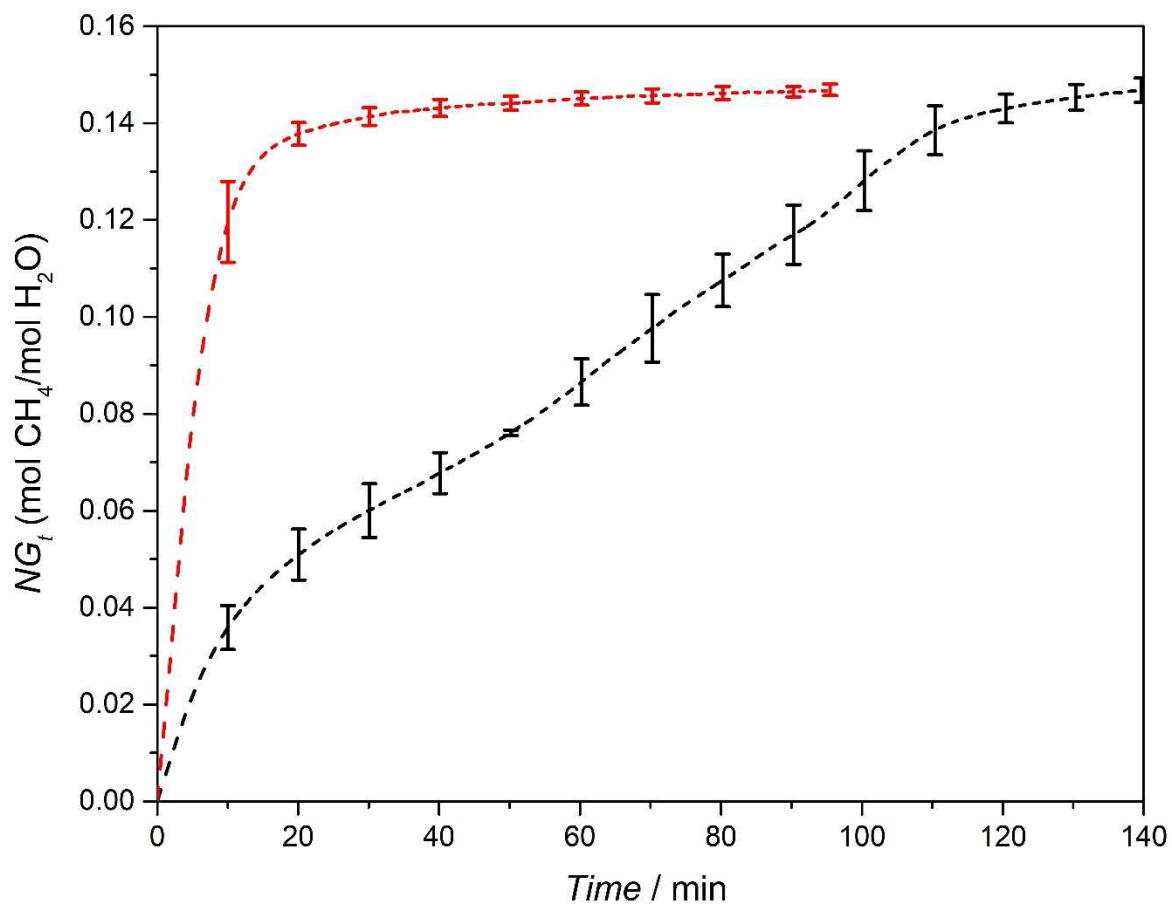
Figure 4. Comparison of CH$_4$ hydrate formation behavior at 273.65 K in 5 mm SSB packed bed (black) and 2 mm SSB packed bed (red) filled with 2.05g H$_2$O. Time zero corresponds to nucleation point
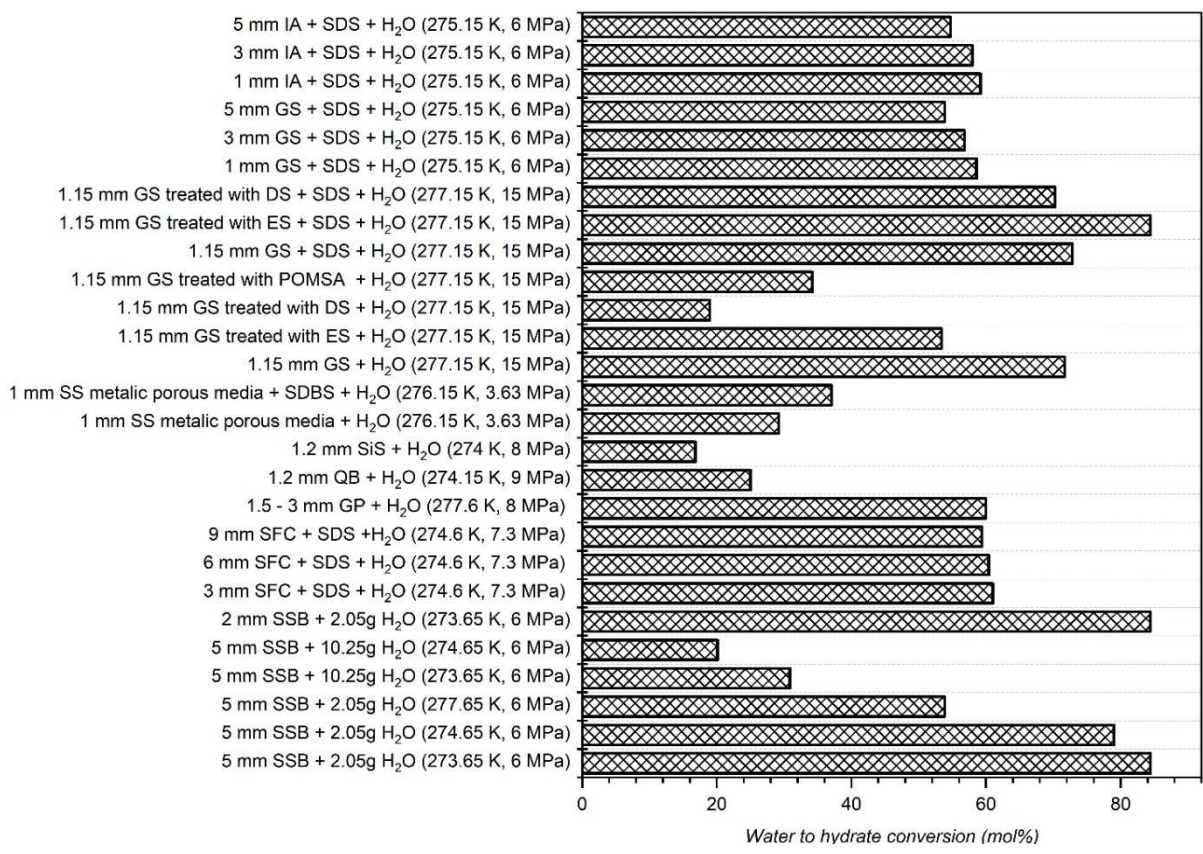
Figure 5. Comparing water to hydrate conversion (mol%) between different fixed packing materials with particle diameters greater than 1 mm (data compiled from [107, 141, 196-200]). IA: inert alumina, GS: glass spheres, ES: ethyltriethoxysilane, DS: *n*-dodecyltriethoxysilane, SDS: sodium dodecyl sulfate, POMSA: peroxymonosulfuric acid, SS: stainless steel, SDBS: sodium dodecyl benzenesulfonate, SiS: Silica sand, GP: granular Pebble, QB: quartz beads, SFC: SiC foam ceramic, SSB: stainless steel beads
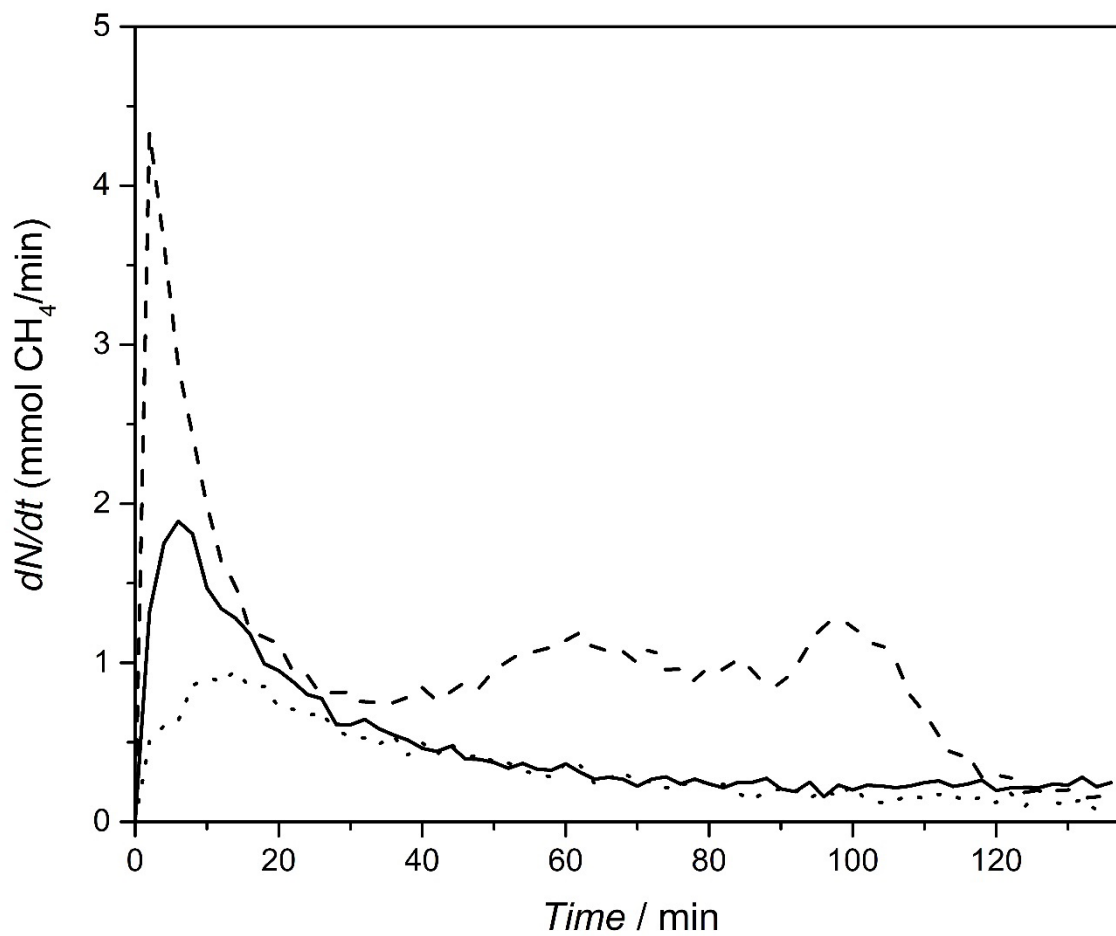
Figure 6. Rate of CH$_4$ hydrate formation at different driving forces; 3.3 MPa (dash), 2.7 MPa (solid), 2 MPa (dot) in 5 mm SSB packed bed filled with 2.05g H$_2$O
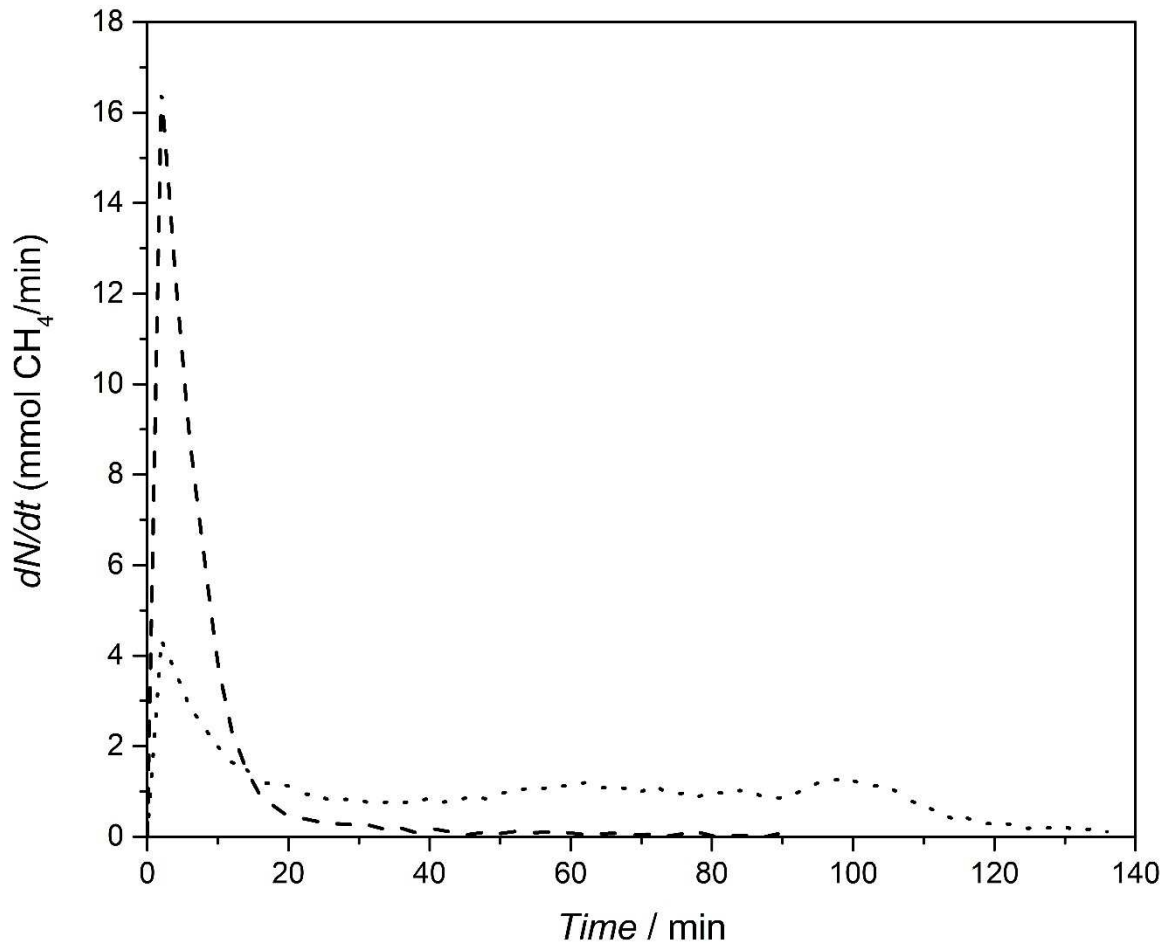
Figure 7. Rate of CH_4 hydrate formation in 2 mm SSB packed (dash) and 5 mm SSB packed (dot) bed filled with 2.05g H_2O at a driving force of 3.3 MPa
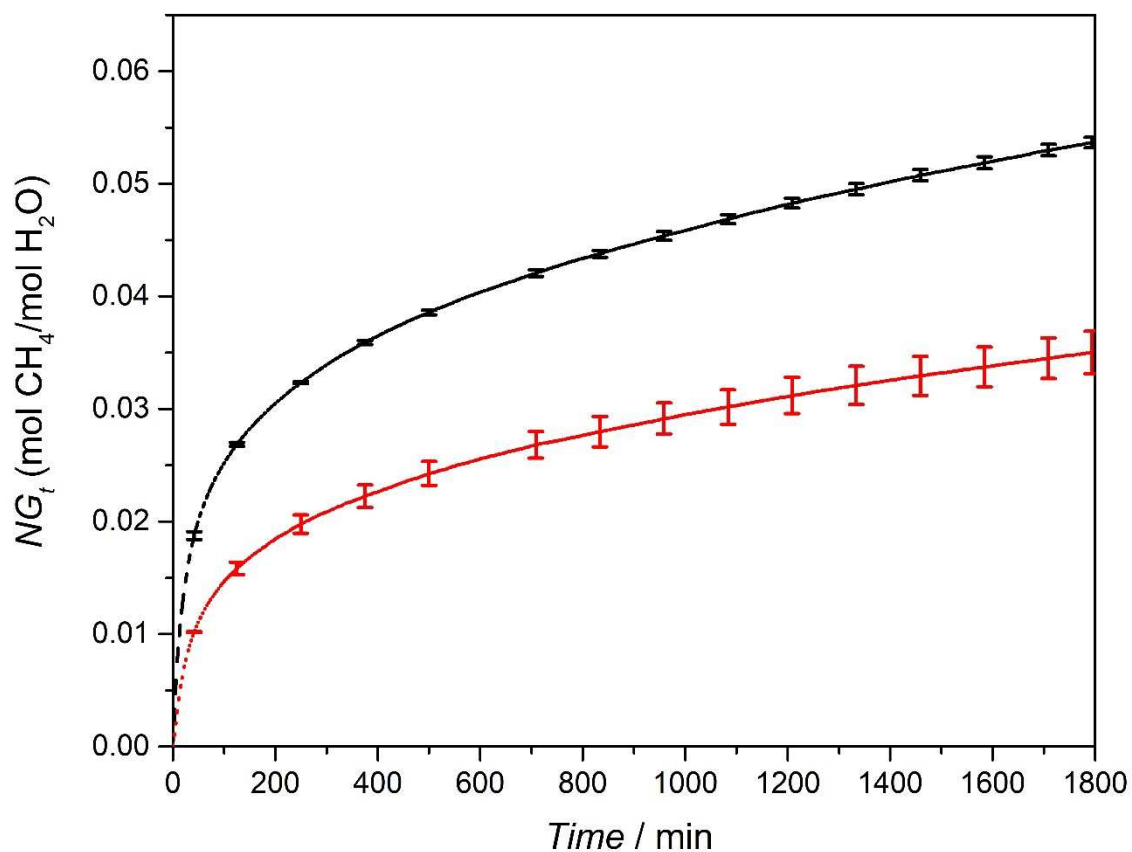
Figure 8. CH₄ gas uptake measurements for the experiments conducted at 273.65 K (black) and 275.65 K (red) in a 5 mm SSB packed bed filled with 10.25g H_2O and with an initial pressure of 6 MPa
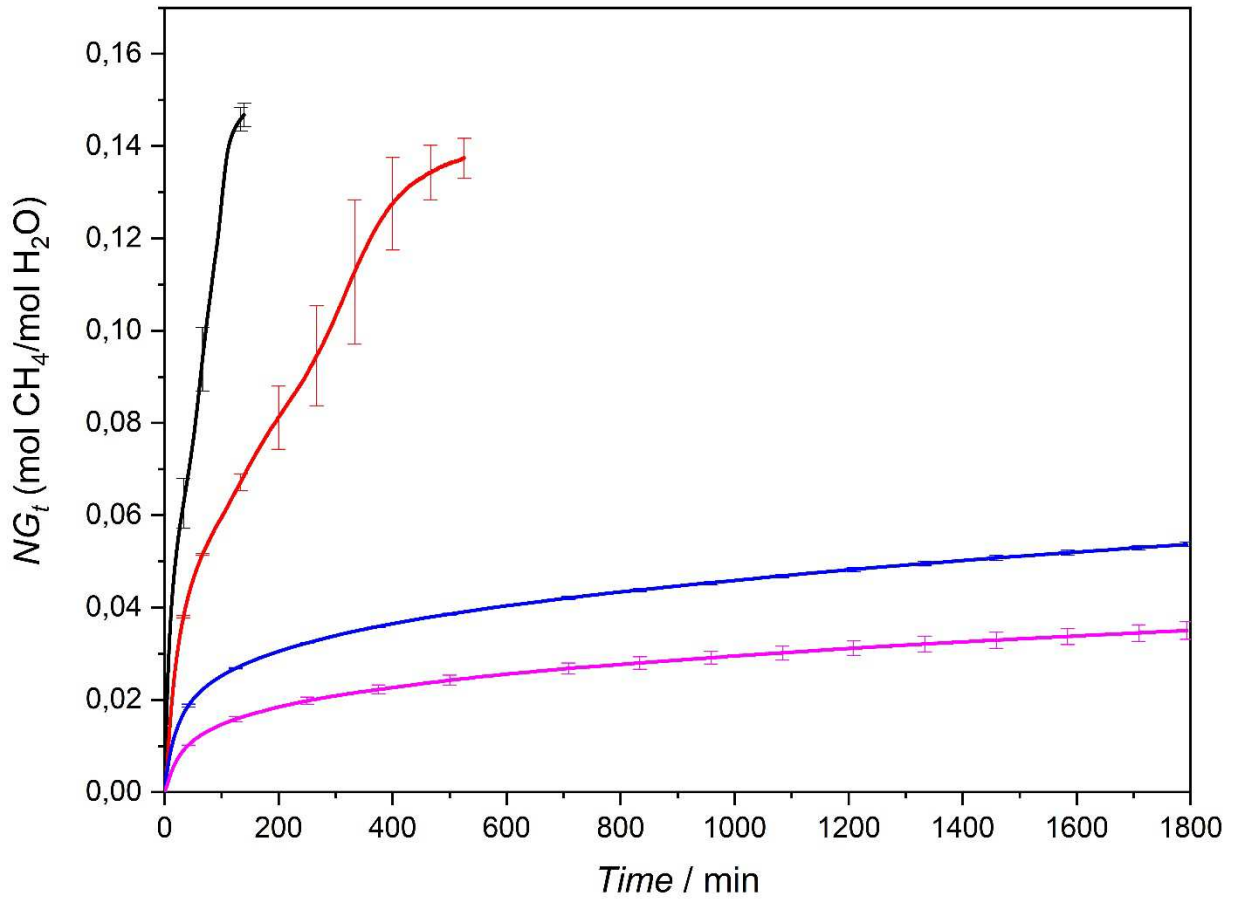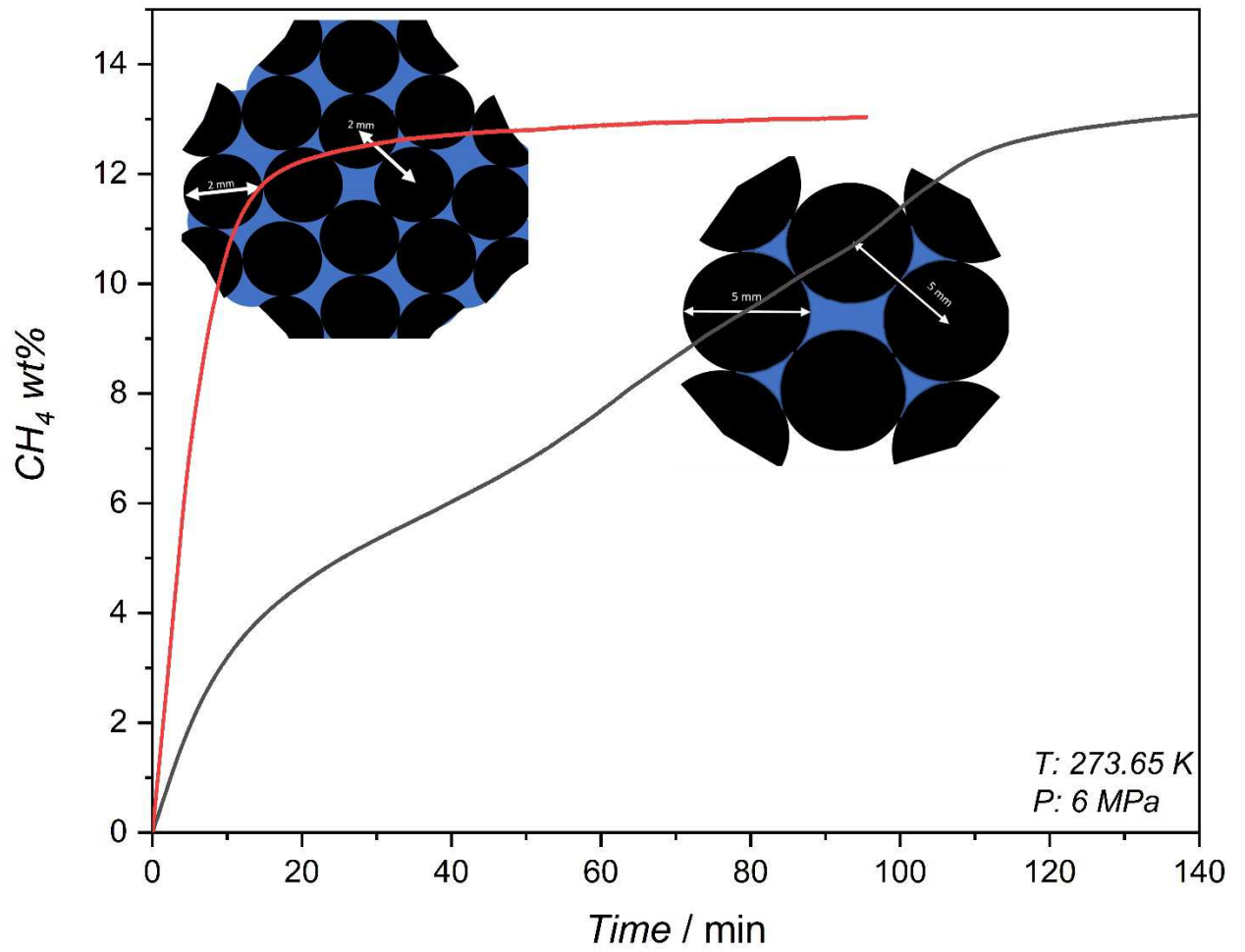
Figure 9. Normalized gas uptake measurements for the experiments conducted at 273.65 K and 275.65 K in a 5 mm SSB packed bed filled with 2.05 g and 10.25 g H_2O. Black: (2.05 g H_2O – 273.65 K), Red: (2.05 g H_2O – 275.65 K), Blue: (10.25 g H_2O – 273.65 K), Magenta: (10.25 g H_2O – 275.65 K)

TOC